Ventral hippocampus-lateral septum circuitry mediates foraging-related spatial memory

Elizabeth A. Davis[1*], Clarissa M. Liu[1,2*], Léa Décarie-Spain[1], Logan Tierno Lauer[1], Isabella H. Gianatiempo[1], Andrea N. Suarez[1], Alyssa M. Cortella[1], Joel D. Hahn[3], and Scott E. Kanoski[1,2]

[*]These two authors contributed equally

[1]Human and Evolutionary Biology Section, Department of Biological Sciences, Dornsife College of Letters, Arts and Sciences, University of Southern California, 3616 Trousdale Pkwy, Los Angeles, CA, USA, 90089; [2]Neuroscience Graduate Program, University of Southern California, 3641Watt Way, Los Angeles, CA, USA. 90089; [3]Neurobiology Section, Department of Biological Sciences, Dornsife College of Letters, Arts and Sciences, University of Southern California, 3616 Trousdale Pkwy, Los Angeles, CA, USA, 90089

Corresponding author:
Scott E. Kanoski, PhD
University of Southern California
3616 Trousdale Parkway, AHF-252
Los Angeles, CA 90089-0372
Phone: 213-821-5762
Email: kanoski@usc.edu

ABSTRACT

Remembering the location of a food or water source is essential for survival. Here we identify a hippocampal-septal neural circuit that is necessary for spatial memory based specifically on appetitive reinforcement. Both reversible and chronic disconnection of ventral hippocampus CA1 subregion (CA1v) projections to the lateral-septum (LS) using pathway-specific dual viral approaches impaired spatial memory retention for the location of either food or water reinforcement. However, disconnection of this pathway did not affect performance in an aversive escape-motivated spatial memory task that used the same apparatus and visuospatial cues. The selectivity of this pathway in mediating foraging-related memory was further supported by results showing that CA1v-LS disconnection did not affect anxiety-like behavior, locomotor activity, or social and olfactory-based appetitive learning. To examine whether CA1v-LS mediation of foraging-related spatial memory involves collateral projections of CA1v neurons, we utilized virus-based neural pathway tracing analyses to identify the medial prefrontal cortex (mPFC) as a collateral target of LS-projecting CA1v neurons. However, functional disconnection of CA1v and mPFC did not affect appetitive spatial memory, thus further supporting the selectivity of CA1v-LS signaling for this behavior. The lateral hypothalamic area, which is associated with food-motivated behavior and more recently with spatial memory, was identified as a second-order target of CA1v-LS signaling using a multisynaptic anterograde tracing approach. Collective results reveal that CA1v to LS communication plays a critical role in remembering an environmental location based on appetitive (food or water) but not aversive (escape) reinforcement, thus identifying a novel neural pathway regulating foraging-related memory processes.

INTRODUCTION

A survival advantage common to early humans and lower-order mammals is to accurately remember the location of a food or water source in the environment, and to then efficiently navigate back to a shelter or other safe location. The neurobiological substrates that regulate visuospatial navigation are therefore critical to effectively implement food-directed or water-directed foraging behavior. In rodents a number of maze tasks have been developed that have been instrumental in identifying brain structures within the telencephalon that are essential for visuospatial mapping and egocentric orientation in the environment, including the hippocampus and the medial entorhinal cortex, respectively (1, 2). However, despite that reliably locating food and water sources in the environment is a key selection pressure driving the evolution of visuospatial navigation, the overwhelming majority of rodent model research on the neural substrates of spatial learning and memory have utilized procedures such as the Morris water maze and the Barnes maze that each involve escaping aversive stimulus conditions (3, 4). Furthermore, while single unit recordings have been used to identify specific populations of neurons that subserve distinct navigational functions (e.g., hippocampal "place cells", medial entorhinal "grid cells") (5, 6), the bulk of this research has recorded neural activity under neutral conditions void of either appetitive or aversive reinforcement. Very little research has been dedicated to identify brain regions and neural circuits that may specifically promote spatial memory based on the location of appetitive reinforcers (e.g., food, water), as well as the extent to which the nature of the reinforcement is a critical factor in deciphering the brain's control of visuospatial navigation.

The majority of rodent model research investigating brain regions that mediate visuospatial navigational memory has focused on the anterior and "dorsal" subregion of the hippocampus (septal pole; HPCd). However, the posterior and "ventral" hippocampus subregion (temporal pole; HPCv), while classically associated with stress- and affect-associated memory processes (7), also plays a role in visuospatial learning and memory (8-10). For example, under some testing conditions selective HPCv lesions impair spatial memory performance in the Morris water maze (10, 11). Moreover, place cells that are responsive to changes in the visuospatial environment are present within both the HPCd and HPCv pyramidal layers, with a linear increase in the spatial scale of representation from the dorsal to the ventral pole (9). Despite a

62 common role for the HPCd and HPCv in mediating spatial memory, there is also evidence for a
63 functional distinction between the subregions (7, 12, 13). For instance, lesions of the HPCv but
64 not the HPCd alter stress responses (14) and anxiety-like behavior (15), whereas HPCd but not
65 HPCv lesions impair spatial memory in an incidental (nonreinforced) procedure (16). These two
66 HPC subregions also have disparate neuroanatomical connectivity supporting a framework for a
67 functional diversity in which the HPCd preferentially processes cortical-derived sensory
68 information and the HPCv preferentially processes metabolic and limbic-derived affective
69 information (7, 13). The functional distinction between these two subregions is further supported
70 by the generation of the hippocampus gene expression atlas, which provides a comprehensive
71 integration of gene expression and connectivity across the HPC septo-temporal axis (17). Given
72 that both the HPCv and the HPCd participate in spatial memory but have distinct
73 neuroanatomical connectivity and contributions when it comes to regulating other cognitive and
74 mnemonic processes, it is feasible that the HPCv and HPCd support different forms of spatial
75 memory depending on the type of reinforcement and/or the context associated with the behavior.
76 Recent findings identify the HPCv as a critical brain substrate in regulating feeding
77 behavior and food-directed memory processes. Reversible inactivation of HPCv neurons after a
78 meal increases the size of and reduces the latency to consume a subsequent meal (18, 19). In
79 addition, receptors for feeding-related hormones are more abundantly expressed in the HPCv
80 compared to the HPCd (e.g., ghrelin receptors (20, 21), glucagon-like peptide-1 [GLP-1]
81 receptors (22)), and these HPCv endocrine and neuropeptide receptor systems alter food intake
82 and feeding-related memory (23-28). Olfactory information, which is intimately connected with
83 feeding behavior, is also preferentially processed within the HPCv compared with the HPCd.
84 The CA1v, specifically, is bidirectionally connected to brain regions that process olfactory
85 information (7, 29, 30), and CA1v neurons respond more robustly to olfactory contextual cues
86 compared with CA1d (8). Given these HPCv appetite-relevant neuroanatomical connections,
87 endocrine and neuropeptide receptor expression profiles, and functional evidence linking this
88 subregion with food-motivated behaviors, we hypothesize that HPCv mediation of visuospatial
89 memory is preferentially biased to food and water-reinforced foraging behavior.
90 HPCv pyramidal neurons have extensive projection targets throughout the brain (31), yet
91 the functional relevance of these pathways is poorly understood. The lateral septum, in
92 particular, is a robust target of HPCv glutamatergic pyramidal neurons (32, 33). Given that this

93 pathway has been shown to affect feeding behavior (34) and that neuroplasticity changes occur
94 in the LS after learning a spatial memory task (35, 36), we hypothesize that that HPCv to LS
95 projections participate in regulating foraging-related spatial memory for food and water location.
96 To investigate this hypothesis, we developed two novel appetitive reinforcement-based spatial
97 foraging behavioral tasks that allow for direct comparison with an aversive reinforcement-based
98 task of similar difficulty that uses the same apparatus and spatial cues. Performance in these
99 tasks was assessed following pathway-specific dual viral-based reversible (chemogenetic
100 inhibition) or chronic (targeted apoptosis) disconnection of the CA1v to LS pathway. To further
101 expand neural network knowledge on CA1v to LS signaling, we used conditional viral-based
102 neuroanatomical tracing strategies to identify both first-order collateral and second-order targets
103 of LS-projecting CA1v neurons. Collective results from the present study identify novel neural
104 circuitry of specific relevance to foraging behavior.
105

RESULTS

The ventral hippocampus (HPCv) is required for remembering the spatial location of food

To examine the importance of the HPCv in memory for the spatial location of food, animals received bilateral *N*-Methyl-D-aspartate excitotoxic lesions of the HPCv (n=12) or bilateral sham injections (control n=12) (histological analyses for the neuron-specific NeuN antigen in Fig. 1A) and were tested in a novel appetitive visuospatial memory task developed in our lab that utilizes a Barnes Maze apparatus. Results revealed no significant differences in errors (incorrect hole investigations) (Fig. 1E) or latency to locate the food source hole (Fig. 1F) during training. However, memory probe results show that animals with HPCv lesions decreased the ratio of correct + adjacent / total holes explored in the first minute compared with controls (Figure 1G; $p<0.05$, cohen's d=-1.0174; analysis for the combined 2-min period did not yield a statistical group difference), indicating impaired memory for the spatial location of food reinforcement.

Post-surgical analyses of food intake (Supp. Fig. 1A) and body weight (Supp. Fig. 1B) found no significant group differences in these measures over time. These collective results indicate the HPCv is required for memory retention but not learning of the spatial location of food in the environment.

Ventral hippocampus CA1 (CA1v) projections to the lateral septum (LS) mediate appetitive spatial memory for food and water location, but not aversive spatial memory for escape location

To identify a specific neural pathway mediating the results described above, we investigated the functional relevance of the CA1v to LS signaling in learning and recalling the spatial location of either food or water reinforcement using conditional dual viral approaches to either reversibly (via cre-dependent pathway-specific inhibitory chemogenetics; diagram of approach in Fig. 2A) or permanently (via cre-dependent pathway-specific caspase-induced lesions; diagram of approach in Fig. 2B) disconnect CA1v to LS communication. Results from the appetitive food seeking spatial memory task reveal no significant group differences during training in either errors before locating the correct hole (Fig. 2E) or latency to locate the food source hole (Fig. 2F). However, memory probe results demonstrate that both acute (pathway-specific DREADDs) and chronic (pathway-specific caspase) CA1v to LS disconnection decreased the ratio of correct

137 + adjacent / total holes explored in the entire two minutes of the probe compared with controls
138 (Fig. 2G; $p<0.05$, cohen's $d=-1.142$; analysis for the 1st minute period alone did not yield a
139 statistical group difference, $p=0.059$), indicating impaired memory for the spatial location of
140 food reinforcement.
141 Results from an analogous appetitive water seeking spatial memory task in a separate cohort of
142 water-restricted rats also reveal no significant group differences during training in either errors
143 before locating the correct hole (Fig. 2H) or latency to locate the food source hole (Fig. 2I).
144 However, a significant impairment was observed following either acute or chronic CA1v to LS
145 disconnection of the ratio of correct + adjacent / total holes explored in 2-min memory probe
146 compared with controls (Fig 2J; $p<0.05$, cohen's $d=-1.18$; analysis for the 1st minute period alone
147 did not yield a statistical group difference), indicating impaired memory for the spatial location
148 of water reinforcement.
149 Histological analyses confirmed successful viral transfection of LS-projecting CA1v
150 neurons with DREADDs (Fig. 2C-D), as well as successful lesioning of LS-projecting CA1v
151 neurons for the caspace approach (Supplemental Fig. 2H-I. The reversible DREADDs-based
152 disconnection approach was further confirmed by c-Fos analyses in the LS, where the number of
153 c-Fos immunoreactive neurons in the LS in response to the food reinforcement-based spatial
154 memory probe test was reduced following CNO treatment relative to vehicle/control treatment
155 (Supp. Fig. 2E-G). Post-surgical analyses of food intake (Supp. Fig 2A) and body weight (Supp.
156 Fig 2B) found no group differences in these measures over time (in the absence of CNO
157 treatment). These data demonstrate that the CA1v-LS disconnection approaches were successful,
158 that CA1v to LS communication is critical for remembering the spatial location of food and
159 water, and that these effects are unlikely to be based on differences in energy status or food
160 motivation.
161 To evaluate whether CA1v to LS signaling is specifically involved in appetitive
162 reinforcement-based spatial memory (food or water) vs. spatial memory in general, in a separate
163 cohort of animals we tested the effect of reversible and chronic CA1v to LS disconnection in a
164 spatial learning task based on aversive reinforcement rather than food. Importantly, this task uses
165 the same apparatus and visuospatial cues as the spatial location food and water memory tasks
166 described above, but the animals are motivated to locate the tunnel to escape mildly aversive
167 stimuli (bright lights, loud noise) with no food or water reinforcement in the tunnel (see Fig. 1B).

168 Training results revealed no significant group differences in errors before correct hole (Fig. 2K)
169 nor latency to locate the escape hole (Fig. 2L). During the memory probe test, there were no
170 group differences in the ratio of correct + adjacent / total holes investigated during the first
171 minute nor the entire two minutes (Fig. 2M) of the memory probe. Post-surgical analyses of food
172 intake (Supp. Fig. 2C) and body weight (Supp. Fig. 2D) found no group differences in these
173 measures over time. These collective findings suggest that CA1v to LS signaling specifically
174 mediates spatial memory in a reinforcement-dependent manner, playing a role in appetitive (food
175 or water reinforcement) but not aversive (escape-based) spatial memory.
176
177 **Reversible, but not chronic disconnection of CA1v to LS signaling increases chow intake**
178 **under free-feeding conditions.**
179 While the results above suggest that the impairments in food or water-based spatial
180 memory were not based on long-term changes in food intake or body weight, these experiments
181 were conducted under conditions of either chronic food or water restriction. To examine the role
182 of CA1v to LS signaling on feeding behavior under free-feeding conditions, we examined meal
183 pattern feeding analyses in the caspase vs. the control group (chronic CA1v-LS disconnection),
184 and in the DREADDs group following CNO or vehicle (within-subjects design; reversible
185 CA1v-LS disconnection). Results averaged over 5d revealed no significant effect of chronic
186 CA1v to LS disconnection (caspase group) on 24h meal frequency, meal size, meal duration, or
187 24h food intake in comparison to controls (Supp. Figs. 3A-D). However, CNO-induced acute
188 reversible silencing of LS-projecting CA1v neurons (DREADDs group) significantly increased
189 24h chow intake (Supp. Fig. 3H; $p<0.05$, cohen's $d=1.0$) relative to vehicle treatment,
190 accompanied by a trend towards increased meal frequency (Supp. Fig. 3E; $p=0.11$) and no effect
191 on meal size or meal duration (Supp. Figs. 3F&G). These results are unlikely based on
192 nonselective effects of the CNO, as we've recently shown that ICV CNO injections do not affect
193 food intake in rats when tested under similar conditions (37). Collectively these findings show
194 that reversible CA1v to LS disconnection increases food intake under free-feeding conditions,
195 whereas food intake is not affected by chronic CA1v to LS ablation.
196
197 **CA1v to LS disconnection does not affect nonspatial HPC-dependent appetitive memory,**
198 **anxiety-like behavior, or levels of locomotor activity**

199 The HPCv plays an important role in the social transmission of food preference
200 procedure (STFP) (28, 38, 39), which tests socially-mediated food-related memory based on
201 previous exposure to socially-communicated olfactory cues (diagram in Fig. 3A). However,
202 results revealed that neither chronic nor acute disconnection of CA1v to LS signaling affected
203 the STFP preference ratio between groups (Fig. 3B), with all three groups performing
204 significantly above chance (based on within-group one sample t-tests, ps<0.05).
205 HPCv to LS circuitry has been shown to play a role in mediating anxiety and stress
206 behavior (40-42). Given that altered anxiety-like behavior and/or locomotion could produce
207 behavioral changes that may lead to an apparent spatial memory deficit in any of the spatial
208 learning tasks used, we examined whether HPCv to LS disconnection yields differences in
209 anxiety-like behavior (zero maze task; diagram of apparatus in Fig. 3C) and/or locomotion (open
210 field test). Zero maze results showed no significant group differences in time spent in the open
211 zones (Fig. 3D) nor in the number of open zone entries (Fig. 3E). In addition, CA1v to LS
212 disconnection had no effect on general locomotor activity in the open field test (Fig. 3F). These
213 collective results suggest that the observed deficits in food- and water-seeking spatial memory
214 are not secondary to impaired nonspatial appetitive learning, general differences in anxiety-like
215 behavior, or locomotor impairments.
216
217 **The medial prefrontal cortex is a collateral target of LS-projecting CA1v neurons**
218 In addition to the LS, CA1v neurons also robustly project to the medial prefrontal cortex
219 (mPFC), a pathway that we have previously shown to be involved in feeding behavior (25). To
220 examine whether LS-projecting CA1v neurons have collateral targets in the mPFC, or in other
221 brain regions, we utilized a conditional dual viral neural pathway tracing approach that identifies
222 collateral targets of a specific monosynaptic pathway (CA1v->LS; diagram of approach in Fig.
223 4A, representative CA1v injection site in Fig. 4B, representative CA1v injection site in Fig. 4C).
224 Results revealed that LS-projecting CA1v neurons also project to the mPFC (Fig. 4D), whereas
225 very minimal labeling was observed in other brain regions throughout the neuraxis. Thus, it may
226 be the case that the impaired spatial memory for food location observed following either
227 reversible or chronic CA1v to LS disconnection are based, in part, on CA1v to mPFC signaling
228 from the same LS-projecting CA1v neurons.
229

230 **CA1v to mPFC signaling does not contribute to appetitive spatial memory**

231 We next sought to test the functional relevance to food-directed spatial memory of a
232 CA1v-originating neural pathway (CA1v to mPFC) that is a collateral target of LS-projecting
233 CA1v neurons. The CA1v to mPFC projections are exclusively ipsilateral (25, 43), and thus this
234 pathway allows for a 'contralesional' approach to achieve complete and chronic functional
235 disconnection (diagram of approach in Fig. 4E&4I, modified from (43)). This approach was
236 utilized in favor of the dual viral approaches used for the CA1v-LS disconnection, as it provides
237 a more complete disconnection between the structures and does not require the use of viruses and
238 involves fewer surgical injections to achieve a similar objective. We note, however, that this
239 contralesional approach is not a feasible option for the CA1v-LS pathway, as CA1v neurons
240 project to the LS bilaterally (e.g., Fig. 5F). Post-surgical analyses of food intake (Supp. Fig. 4A)
241 and body weight (Supp. Fig. 4B) found no group differences in these measures over time
242 between sham controls and the chronic CA1v-mPFC disconnection group. Training results from
243 the appetitive spatial memory task revealed no group differences in errors before locating the
244 correct hole (Fig. 4F or latency to locate the food-baited hole (Fig. 4G). Importantly, memory
245 probe results demonstrate that CA1v to mPFC disconnection did not alter the ratio of correct +
246 adjacent / total holes explored in the first minute or the entire two minutes (Fig. 4H, 4L)
247 compared with controls. These data collectively demonstrate that CA1v to LS mediation of
248 foraging-related memory does not require collateral projections to the mPFC neural pathway.
249

250 **LS neurons activated during appetitive spatial memory testing are primarily GABAergic**

251 Fluorescent *in situ* hybridization analyses were used to determine the neurotransmitter
252 phenotype cFos+ LS neurons that were activated during the appetitive food seeking spatial
253 memory probe test. Results revealed that ~10% of c-Fos+ LS neurons express ChAT (a
254 cholinergic marker; Fig. 5A), ~88% of cFOS+ LS neurons express GAD1 (a GABAergic; Fig.
255 5B), and only ~2% of cFOS+ LS neurons express VGLUT2 (a glutamatergic marker; Fig. 5C).
256 These results suggest that LS neurons engaged during the spatial memory probe are primarily
257 GABAergic (Fig. 5D).
258

259 **The lateral hypothalamic area (LHA) is a primary second-order target of LS neurons that**
260 **receive CA1v input**

261 A dual viral tracing strategy (diagram of approach in Fig. 6A; representative LS injection
262 site in Fig. 6B) was utilized to identify downstream targets of LS-projecting CA1v neurons.
263 Results revealed that the LHA is the strongest second-order target of the CA1v to LS-projecting
264 neurons (Fig. 6C-D). Quantitative analyses using a custom-built data-entry platform (Axiome C,
265 created by JDH) are summarized graphically for a representative animal on a brain flatmap
266 summary diagram (Fig. 6D) for the hemisphere ipsilateral (top) and contralateral (bottom) to the
267 injection sites (see Supplementary Table 1 for data from complete forebrain analyses).
268 Retrograde transfection of the AAVs from the injection sites was not observed, as tdTomato+
269 cell bodies were only observed in the LS following complete forebrain histological analyses.
270 Additional confirmation of the LHA as a second-order target was provided via a co-injection
271 (COIN) strategy, from (44, 45). This approach involved injections of a monosynaptic retrograde
272 tracer, fluorogold (FG), in the LHA (representative injection site in Fig. 6E) and injection of a
273 monosynaptic anterograde tracer, AAV1-GFP, in the CA1v (representative injection site in Fig.
274 6F), which resulted in the observance of FG-GFP appositions in the LS to further confirm this
275 multisynaptic pathway (Fig. 6G).
276
277
278 **DISCUSSION**
279
280 Memory for the physical location of a food or water source is adaptive for maintaining
281 adequate energy supply for reproduction and survival. However, the neural circuits mediating
282 this complex behavior are not well understood as research on visuospatial memory has
283 predominantly used tasks with either aversive or neutral/passive reinforcement. Moreover,
284 whether the neural circuitry mediating spatial memory function is divergent based on the nature
285 (e.g., appetitive vs. aversive) or modality (e.g., food vs. water) of the reinforcement has not been
286 systematically investigated. The present study identified a monosynaptic CA1v to LS pathway as
287 a necessary substrate for food- and water-motivated spatial memory. Moreover, the selectivity of
288 the CA1v-LS pathway in mediating spatial memory for food and water location is supported by
289 results showing that disconnection of this pathway did not affect performance in an escape-
290 motivated spatial memory task of comparable difficulty conducted in the same apparatus,
291 anxiety-like behavior, locomotor activity, or olfactory and social-based appetitive memory.
292 Fluorescent in situ hybridization analyses also demonstrate that LS neurons engaged during

293 appetitive spatial memory testing are primarily GABAergic. Viral-based pathway tracing
294 revealed that LS-projecting CA1v neurons also send collateral projections to the mPFC,
295 however, functional disconnection of CA1v-mPFC signaling did not impair spatial memory for
296 food location. Utilization of an anterograde multisynaptic viral tracing approach and quantitative
297 forebrain-wide axon mapping analyses revealed that the CA1v-LS pathway sends second-order
298 projections to various feeding and reward-relevant neural substrates, particularly the LHA.
299 Collectively, these data establish monosynaptic CA1v to LS signaling as an essential pathway for
300 spatial memory-based foraging behavior, and we further identify a neural network of
301 interconnected feeding-relevant substrates that are collateral and/or downstream targets of this
302 pathway.

303 Historically, the hippocampus has been divided into the dorsal and ventral subregions
304 that have both distinct and overlapping functions, anatomical connections, and genetic and
305 receptor expression profiles (12, 13, 17, 31, 46). The HPCd has been predominantly implicated
306 in facilitating spatial memory, whereas the HPCv is linked more with stress responses, affective
307 behavior, and energy balance. However, a recent study found that both the HPCd and HPCv
308 were critical for food reward-directed spatial navigation in an obstacle-rich complex
309 environment (47), and under certain testing conditions, spatial learning and memory in an
310 aversive reinforcement-based water maze also requires both subregions of the HPC (48). Here
311 we expand this literature by identifying a specific HPCv-originating pathway (CA1v->LS) that
312 selectively mediates spatial memory for the location of appetitive (food or water) reinforcement.
313 These novel findings suggest that the modality of the reinforcement should be considered when
314 investigating the longitudinally-organized processing of spatial information across the dorsal-
315 ventral HPC axis.

316 While HPCv neurons project widely throughout the neuraxis, projections to the LS are
317 particularly robust (33). The LS has been implicated in food anticipatory/seeking behavior,
318 where metabolic activation of the lateral septum peaks immediately before feeding (during food
319 anticipatory activity) in rabbit pups (49) and gamma-rhythmic input to the LHA from the LS
320 evokes food approach behavior (50). In addition, the LS can bidirectionally modulate food intake
321 via a number of feeding-relevant neuropeptides, including glucagon-like peptide-1, ghrelin, and
322 urocortin (51-53). Recent findings demonstrate that DREADDs-mediated disconnection of a
323 HPCv to LS pathway (from CA3v and DGv) increases food intake in mice, with

opposite/hyperphagic effects observed following activation of this pathway (34). Similarly, here we demonstrate that DREADDs-mediated acute silencing of the CA1v to LS pathway increases food intake in rats. Together these findings support a role for HPCv-LS signaling in regulating eating behavior. However, these results are based on analyses conducted in the home cage where animals have free and unlimited access to food and water. Here we extend these findings by establishing a role of CA1v to LS signaling in foraging-relevant memory processes under conditions that are more relevant to normal mammalian behavior, where food and water are not freely available.

The use of two different but complementary approaches for neural pathway-specific disconnection allowed us to test at the levels of learning and memory separately. For example, the use of a reversible (DREADDs) disconnection procedure allowed us to evaluate the effect of CA1v to LS disconnection during the memory probe only, with circuit intact during training (CNO was not administered at any point during training). In contrast, the chronic (caspase) disconnection procedure was performed before training and therefore could have affected learning if CA1v to LS pathways were required for the learning of the task. However, our results showed that CA1v to LS disconnection did not impair learning, but rather, only memory retention performance in the probe test conducted days after the end of training. Thus, we can now confirm based on two complementary levels of analysis that this pathway is involved in longer-term memory recall but not learning/acquisition, which is consistent with recent evidence demonstrating that complete HPCv lesions impair retrieval (probe performance), but not acquisition (learning) in a Morris water maze (54). A limitation of the present study is that we did not evaluate 'gain of function' of CA1v->LS signaling on appetitive spatial memory. However, we note that such gain of function approaches are more commonly utilized with models of memory dysfunction. Thus, an important area for follow-up research is to investigate whether enhanced CA1v->LS signaling (e.g., via excitatory pathway-specific DREADDs) can augment memory function in models where foraging-related memory is impaired.

While the use of aversive reinforcement-based spatial memory tasks are predominant in the field, the radial arm maze has also been used to investigate food-motivated spatial memory (55). Common applications include win-shift tasks, where animals learn to avoid previously visited food-baited arms (working memory, modeling spontaneous alternation and exploration in environments with minimal resources), and win-stay tasks where animals learn to return to

355 previously reinforced arms modeling foraging in environments of plentiful resources (reference
356 memory). Our experiments are analogous to the latter. However, an advantage of the present
357 food-reinforced Barnes Maze apparatus-based approach over the radial arm maze procedure is
358 that we've developed parallel procedures that use the same apparatus and visuospatial cues to
359 examine water- and escape-motivated spatial memory, thus offering a unique arsenal to assess
360 the selectivity of the circuit based on multiple reinforcement modalities (food vs. water vs.
361 escape/aversive). Future research is needed to determine whether CA1v to LS signaling also
362 mediates spatial working memory based on appetitive and/or aversive reinforcement.
363 Utilizing dual viral approaches and systematic forebrain-wide quantitative mapping
364 analyses, our findings confirm that the CA1v-LS pathway projects downstream to other neural
365 substrates involved in feeding and motivated behavior, including the LHA, ACB, and mPFC.
366 This experiment was performed to generate novel neural connectivity data for the field and to
367 demonstrate possible downstream 2nd-order targets that may inspire future research focused on
368 these newly-identified multi-order neural circuits. We identified the LHA as the most robust
369 downstream 2nd-order target of CA1v->LS signaling, and this multisynaptic pathway was
370 corroborated by an additional monosynaptic tracing approach that combined retrograde tracing
371 (FG in LHA) and anterograde tracing (AAV1-GFP in CA1v) to confirm a connection relay in the
372 LS. While future research is required to test the functional relevance of this multisynaptic
373 pathway to appetitive foraging-relevant memory, we hypothesize that the LHA is a functional
374 downstream target based on recent findings linking LHA neurons with spatial memory (56).
375 Collective results identify a CA1v to LS pathway involved in food- and water-motivated
376 spatial memory, but not escape-motivated spatial memory. Furthermore, the selectivity of this
377 pathway to appetitive spatial memory is supported by data showing that neither chronic nor
378 reversible disruption of CA1v to LS signaling influenced various other behavioral outcomes,
379 including anxiety-like behavior, locomotor activity, and nonspatial HPC-dependent appetitive
380 memory. We also systematically characterized collateral and second-order projections of this
381 pathway. Present results demonstrate overlapping pathways coordinated in the higher-order
382 control of energy balance, of which foraging behavior is an essential component given that
383 foraging requires energy expenditure to locate food for subsequent energy intake. These data
384 shed light on the neural systems underlying complex learned and motivated behaviors that
385 require functional connections between cognitive and feeding-relevant substrates.

386 **MATERIALS AND METHODS**

387

388 **Animals**

389 Adult male Sprague–Dawley rats (Envigo; 250-275g on arrival) were individually housed
390 in hanging wire cages with *ad libitum* access (except where noted) to water and chow (LabDiet
391 5001, LabDiet, St. Louis, MO) on a 12h:12h reverse light/dark cycle. All procedures were
392 approved by the University of Southern California Institute of Animal Care and Use Committee.

393

394 **Acute and chronic disconnection of the CA1v to LS neural pathway**

395 Cre-dependent dual viral strategies were used to generate the following groups: [1] acute
396 chemogenetic disconnection of the CA1v to LS neural pathway (DREADDs; diagram of
397 approach in Fig. 2A), [2] chronic disconnection of the CA1v to LS neural pathway (caspase
398 lesion-induced; diagram of approach in Fig. 2B), and [3] a common/shared control group for
399 these two disconnection strategies. Regardless of group, all animals received a bilateral AAV
400 retro-cre injection in the LS (AAV2[retro]-hSYN1-EGFP-2A- iCre-WPRE; 200nL per side) at
401 the following stereotaxic coordinates (57): +0.84mm AP, +/-0.5mm ML, −4.8mm DV, all
402 defined at bregma.

403 According to experimental group, animals received a different virus delivered to the
404 CA1v subregion of the HPCv. All viruses were administered to the CA1v at the following
405 stereotaxic coordinates (57): −4.9mm AP defined at bregma, +/-4.8mm ML defined at bregma,
406 −7.8mm DV defined at skull surface at target site.

407 *[1] DREADDs group for reversible inactivation of CA1v to LS:* To allow reversible
408 chemogenetic inactivation of the CA1v to LS neural pathway, one group of animals received a
409 bilateral CA1v injection of a cre-dependent virus to drive expression of inhibitory designer
410 receptors activated by designer drugs (DREADDs), (AAV-Flex-hm4Di-mCherry). This dual
411 viral strategy drives expression of inhibitory DREADDs exclusively in LS-projecting CA1v
412 neurons, which enables acute inactivation of these neurons by injection of the DREADDs ligand,
413 clozapine-N-oxide (CNO), at the time of behavioral testing.

414 *[2] Caspase group for chronic inactivation of CA1v to LS:* To allow chronic
415 disconnection of the CA1v to LS neural pathway, a second group of animals received a bilateral
416 CA1v cre-dependent caspase virus (AAV1-Flex-taCasp3-TEVp; 200nL per side) mixed with a

417 cre-dependent reporter virus (AAV-flex-tdTomato; 200nL per side) for histological verification.
418 This dual viral strategy drives expression of the apoptosis-mediator molecule caspase exclusively
419 in LS-projecting CA1v neurons, which induces apoptotic cell death in these neurons while
420 leaving other CA1v neurons intact.

421 *[3] Common control:* A common control group was generated so that the DREADDs and
422 caspase groups could both be compared to the same control group, instead of two different
423 control groups for the DREADDs and caspase groups, respectively. This allowed us to reduce
424 the number of animals needed for the same experimental objective. Thus, all animals received an
425 indwelling cannula and ICV injections of CNO as described below.

426 Immediately following viral injections, all animals were surgically implanted with a
427 unilateral indwelling intracerebroventricular (ICV) cannula (26-gauge, Plastics One, Roanoke,
428 VA) targeting the lateral ventricle (VL). Cannulae were implanted and affixed to the skull with
429 jeweler's screws and dental cement at the following stereotaxic coordinates: −0.9mm AP defined
430 at bregma, +1.8mm ML defined at bregma, −2.6mm DV defined at skull surface at site.
431 Placement for the VL cannula was verified by elevation of blood glucose resulting from an
432 injection of 210µg (2µL) of 5-thio-D-glucose (5TG) using an injector that extended 2mm beyond
433 the end of the guide cannula (58). A post-injection elevation of at least 100% of baseline
434 glycemia was required for subject inclusion. Animals that did not pass the 5TG test were retested
435 with an injector that extended 2.5mm beyond the end of the guide cannula and, upon passing the
436 5TG test, were subsequently injected using a 2.5mm injector instead of a 2mm injector for the
437 remainder of the study. Prior to behavioral testing where noted, all animals received an ICV
438 18mmol infusion (2uL total volume) of the DREADDs ligand clozapine N-oxide (CNO) (59),
439 rendering only DREADDs animals chemogenetically inactivated. CNO injections were hand
440 delivered using a 33-gauge microsyringe injector attached to a PE20 catheter and Hamilton
441 syringe through the indwelling guide cannulae. Injectors were left in place for 30sec to allow for
442 complete delivery of the CNO.

443 Cre-dependent DREADD expression targeting LS-projecting neurons in CA1v was
444 evaluated based on localization of the fluorescent reporter mCherry. Immunohistochemistry for
445 red fluorescent protein (RFP) was conducted to amplify the mCherry signal (see
446 Immunohistochemistry). Only animals with mCherry expression restricted within CA1v neurons
447 were included in subsequent behavioral analyses. Representative images in Figs. 2C&D.

448 The general approach for neuronal apoptosis due to activation of cre-dependent caspase
449 targeting LS-projecting neurons in CA1v was validated in a separate cohort (n=8) based on
450 reduction of a cre-dependent fluorescent reporter tdTomato due to neuron cell death compared
451 with controls. The caspase group brains (which received a retro-cre virus in the LS in
452 conjunction with an injection of cre-dependent caspase virus mixed with a cre-dependent virus
453 that drives a tdTomato fluorescent reporter in the CA1v) were compared to control brains (that
454 received a retro-cre virus in the LS in conjunction with only a cre-dependent that drives a
455 tdTomato fluorescent reporter in the CA1v, which was equivalently diluted to match the caspase
456 injections). In both groups, immunohistochemistry for red fluorescent protein (RFP) was
457 conducted to amplify the tdTomato signal (see Immunohistochemistry). Confirmation of
458 successful caspase-driven lesions in the CA1v using this approach was evaluated by reduced
459 tdTomato fluorescence in comparison to control animals, with the expression of CA1v tdTomato
460 expression in the caspase group less than 15% of that observed in controls, on average
461 (Representative images in Supplementary Fig.2 H-I). While this cohort allowed for successful
462 validation of the pathway-specific disconnection caspase approach, to improve the viability of
463 the animals for long-term behavioral analyses, the 3rd AAV with the fluorescent reporter (cre-
464 dependent tdTomato AAV) was omitted for cohorts undergoing behavioral analyses. For these
465 groups, histological confirmation for inclusion in subsequent statistical analyses was based on
466 identification of injections sites confined with the LS and CA1v, as observed using darkfield
467 microscopy.
468
469 **Appetitive food seeking spatial memory task**
470 To test visuospatial learning and memory for food reinforcement, we developed a novel
471 spatial food seeking task modified from the traditional Barnes maze procedure (4). Throughout
472 this paradigm, animals were maintained at 85% free-feeding body weight. The procedure
473 involves an elevated gray circular platform (diameter: 122cm, height: 140cm) consisting of 18
474 uniform holes (9.5cm diameter) spaced every twenty degrees around the outside edge. Under one
475 of the holes is a hidden tunnel (38.73cm L x 11.43cm W x 7.62cm D and a 5.08cm step).
476 Surrounding the table are distinct spatial cues on the wall (e.g., holiday lights, colorful shapes,
477 stuffed unicorn) that are readily visible to the animal. In contrast to the traditional Barnes Maze
478 where an animal uses the spatial cues to escape mildly aversive stimuli in the environment (e.g.

479 bright light and loud sound), this task utilizes food as motivation, such that each hidden tunnel
480 contained five 45mg sucrose pellets (Bio-Serv, Flemington, NJ). Additionally, a quiet white
481 noise (60dB) was used to drown out background noise and floor lamps were used for low-level
482 ambient lighting. On the first day, each animal underwent a habituation session consisting of
483 1min inside a transport bin under the table, 2min underneath the start box in the center of the
484 table, and 3 min inside the hidden tunnel with 5 sucrose pellets. During training, each rat was
485 assigned a specific escape hole according to the position of the spatial cues with the location
486 counterbalanced across groups. Before each trial, animals were placed in the start box for 30
487 seconds. Animals were trained over the course of two 5-min trials per day for four days (five
488 days in contralesional experiments) to learn to use the spatial cues in order to locate the correct
489 hole with the hidden tunnel with sucrose pellets. After finding the correct hole and entering the
490 hidden tunnel during each 5min training session, animals were allowed to remain in the hidden
491 tunnel for 1 minute, and consistently consumed all 5 sucrose pellets at this time. In the event that
492 a rat did not find the correct hole during the 5min training session, the experimenter gently
493 guided the rat to the correct hole and were allowed to crawl in and then complete the training in
494 the same fashion as rats that found the hole on their own. Learning during training was scored
495 via animal head location tracking by AnyMaze Behavior Tracking Software (Stoelting Co.,
496 Wood Dale, IL). The incorrect hole investigations prior to finding the correct hole with sucrose
497 pellets ("errors before correct hole") as well as time to finding the correct hole ("latency to
498 correct hole") were calculated as an average of the two trials per day, and examined across days
499 of training.
500 After the conclusion of training, rats had a two-day break where no procedures occurred,
501 then were tested in a single 2min memory probe in which the hidden tunnel and sucrose pellets
502 were been removed. All animals received an ICV 18mmol infusion of CNO (2uL total volume)
503 1h prior to the memory probe, rendering only DREADDs animals chemogenetically inactivated
504 by CNO. In the memory probe, the ratio of the correct hole plus adjacent hole investigations over
505 the total number of hole investigations were calculated via animal head location tracking by
506 AnyMaze Behavior Tracking Software (Stoelting, Wood Dale, IL). This dependent variable was
507 selected a priori instead of correct hole only investigations based on recent findings
508 demonstrating that taste-responsive hippocampal neurons exhibit weaker spatial selectivity in
509 comparison to non-taste-responsive hippocampal neurons (60). When establishing and refining

510 the food-reinforced spatial memory procedure in multiple cohorts of rats, our preliminary data
511 revealed that memory probe effects in normal/control animals are either stronger in the 1st
512 minute, or in the 1st two minutes combined (but not the 2nd minute alone), with some cohorts
513 showing larger paradigm effects in minute 1, and others in minutes 1+2. Thus, for all
514 experiments presented we analyzed both the 1st minute and the 1st two minutes combined based
515 on an a priori determination from our preliminary studies. A diagram of the apparatus used for
516 the spatial foraging task is included in Fig. 1B.
517 During training sucrose pellets were taped underneath all of the holes to preclude
518 olfactory-based search strategies during training. Importantly, the memory probe test does not
519 include any sucrose pellets in the apparatus at all, and therefore there is no possibility of sucrose
520 odor cues to influence memory probe performance.
521
522 **Appetitive water seeking spatial memory task**
523 We modified our spatial food seeking task to utilize water reward instead of food reward.
524 Throughout this paradigm, animals were water restricted and received 90-min access to water
525 daily (given at least 1hr after the termination of behavioral procedures each day). In addition to
526 the habituation parameters described above, animals in this task were subjected to two 10-min
527 habituation sessions in the hidden tunnel with a full water dish prior to training, which allowed
528 them to become accustomed to reliably drinking from the water dish in the hidden tunnel.
529 Training procedures were the same as for the food-based task above, except instead of sucrose
530 pellets in the hidden tunnel, a water dish containing ~100 mL of water was placed in the back of
531 the hidden tunnel during training, and animals were allowed to remain in the hidden tunnel for
532 2min (instead of 1min, as above). Each animal consumed a minimum of 2mL of water during
533 this time for the training sessions. This newly-developed procedure allowed us to test spatial
534 learning and memory motivated by water reward using similar apparatus and stimulus conditions
535 to the food-reinforced task.
536
537 **Aversive spatial memory escape task (Barnes maze)**
538 To test visuospatial learning and memory for escape reinforcement, we used a modified
539 traditional Barnes maze procedure, which is a visuospatial-based escape task (4). Procedures
540 were exactly the same as above (appetitive spatial memory food seeking and water seeking tasks,

541 using the same apparatus, in the same room, and with the same visuospatial cues) aside from the
542 omission of the sucrose pellets or water dish in the hidden tunnel, the presence of mildly aversive
543 bright (120W) overhead lighting instead of dim ambient lighting, and a mildly aversive loud
544 white noise (75dB) instead of a quiet white noise (60dB). This allowed us to test spatial learning
545 and memory motivated by escape from aversive stimuli in a nearly-identical procedure to our
546 spatial foraging test for learning and memory motivated by palatable food or water consumption.
547 A diagram of the apparatus used for the spatial escape task is included in Fig. 1B.
548
549 **General intracranial injection procedures**
550 Rats were anesthetized via an intramuscular injection of an anesthesia cocktail (ketamine
551 90mg/kg body weight [BW], xylazine, 2.8mg/kg BW and acepromazine and 0.72mg/kg BW)
552 followed by a pre-operative, subcutaneous injection of analgesic (ketoprofen, 5mg/kg BW). Post-
553 operative analgesic (subcutaneous injection of ketoprofen, 5mg/kg BW) was administered once
554 per day for 3 days following surgery. The surgical site was shaved and prepped with iodine and
555 ethanol swabs, and animals were placed in a stereotaxic apparatus for stereotaxic injections.
556 NMDA or viruses were delivered using a microinfusion pump (Harvard Apparatus, Cambridge,
557 MA, USA) connected to a 33-gauge microsyringe injector attached to a PE20 catheter and
558 Hamilton syringe. Flow rate was calibrated and set to 83.3nl/sec. Injectors were left in place for
559 2min post-injection to allow for complete delivery of the infusate. Specific viruses/drugs,
560 coordinates, and injection volumes for procedures are detailed below. Following the completion
561 of all injections, incision sites were closed using either surgical staples, or in the case of
562 subsequent placement of an indwelling cannula, simple interrupted sutures. Upon recovery from
563 anesthesia and return to dorsal recumbency, animals were returned to the home cage. All
564 behavioral procedures occurred 21 days after injections to allow for complete transduction and
565 expression of the viruses, or complete lesioning drugs. General intracranial injection procedures
566 were followed for all injection procedures below.
567
568 **Chronic lesions of the HPCv**
569 Lesion animals received bilateral excitotoxic HPCv lesions via intracranial injections of
570 N-methyl-d-aspartate (NMDA; 4ug in 200nL; 100uL per hemisphere) at the following
571 coordinates at three different sites along the rostrocaudal extent of the HPCv (57): [1] -4.8mm

572 AP, +/-5.0mm ML, -7.5mm DV, [2] -5.5mm AP, +/-4.5mm ML, -7.0mm DV, and [3] -6.1mm
573 AP, +/-4.8mm ML, -7.0mm DV with control animals receiving vehicle saline in the same
574 location. The reference points for AP and ML coordinates were defined at bregma, and the
575 reference point for the DV coordinate was defined at the skull surface at the target site.
576 Bilateral HPCv lesion brains were histologically evaluated for the correct placement of
577 lesions in 1 out of 5 series of brain tissue sections. Neurons were visualized using
578 immunohistochemistry for the neuron specific antigen NeuN (see Immunohistochemistry). The
579 extent of NMDA lesions was determined postmortem by immunohistochemical detection of the
580 neuronal marker NeuN. Rats showing pronounced (~65%) loss of NeuN labeling within the
581 target region compared with the representative NeuN expression following sham injections in the
582 control group (average HPCv count of NeuN+ cells in control group) were included in data
583 analysis (43). Representative images in Fig. 1A.
584
585 **Contralesional disconnection of the CA1v to mPFC neural pathway**
586 To functionally disconnect the CA1v to mPFC pathway (diagram of approach in Fig. 4E),
587 lesion animals received a unilateral excitotoxic CA1v lesion via an intracranial injection of
588 NMDA (200nL) at the following coordinates (33): −4.9mm AP defined at bregma, + or - 4.8mm
589 ML defined at bregma (left/right counterbalanced to be contralateral to mPFC or LHA lesion
590 within-animal), −7.8mm DV defined at skull surface at site, with control animals receiving
591 vehicle saline injections in the same location.
592 In addition to the CA1v lesion, CA1v to mPFC disconnect animals also received a
593 unilateral excitotoxic mPFC lesion via two intracranial injections of NMDA (4ug in 200nL;
594 100nL per injection) at the following coordinates (57): [1] +2.7mm AP, + or - 0.7mm ML
595 (left/right counterbalanced to be contralateral to CA1v lesion within-animal), −5.3mm DV and
596 [2] +3.0mm AP, + or - 0.7mm ML (left/right counterbalanced to be contralateral to CA1v lesion
597 within-animal), −4.7mm DV, with control animals receiving vehicle saline in the same location.
598 The reference points for all mPFC coordinates were defined at bregma.
599 Contralesional brains were histologically evaluated for the correct placement of lesions by
600 visualizing neurons using immunohistochemistry for the neuron specific antigen NeuN (see
601 Immunohistochemistry). The extent of NMDA lesions was determined postmortem by
602 immunohistochemical detection of the neuronal marker NeuN. Rats showing pronounced (65%)

603 loss of NeuN labeling within the target region compared with a sham injection in the
604 contralateral side were included in data analysis (43).
605
606 **Food intake and body weight**
607 For the day prior to surgery (day 0) and for two weeks thereafter, 24h chow intake was
608 measured daily just prior to dark cycle onset to determine effects of experimental procedures on
609 food intake. Spillage was accounted for daily by collecting crumbs onto Techboard paper placed
610 under the cages of each animal. Additionally, animals were weighed daily just prior to dark cycle
611 onset to determine effects of experimental procedures on body weight.
612
613 **Meal pattern**
614 Meal size, meal frequency, meal duration, and cumulative 24h food intake were
615 measured using Biodaq automated food intake monitors (Research Diets, New Brunswick, NJ).
616 Rats (control n=7, caspase n=8, and DREADDs n=8) were acclimated to the Biodaq on ad
617 libitum chow for 3 days. Caspase group vs. control group feeding behavior data were collected
618 over a 5-day period (untreated, between-subjects design). The DREADDs group was tested using
619 a 2-treatment within-subjects design. Rats received 18mmol infusion of ICV CNO (2uL total
620 volume) or vehicle (daCSF, 33% dimethyl sulfoxide in artificial cerebrospinal fluid) 1h prior to
621 lights off and 24h feeding behavior was measured. Meal parameters were set at minimum meal
622 size=0.2g and maximum intermeal interval=600s.
623
624 **Social transmission of food preference (STFP)**
625 To examine food-related memory based on social- and olfactory-based cues, we utilized
626 the social transmission of food preference (STFP) task and adapted protocols from (28, 39, 61,
627 62). Briefly, untreated normal adult rats are designated as 'Demonstrators', while experimental
628 groups are designated as 'Observers'. Demonstrators and Observers are habituated to a powdered
629 rodent chow [LabDiet 5001 (ground pellets), LabDiet, St. Louis, MO] overnight. 24h later,
630 Observers are individually paired with demonstrators and habituated to social interaction, where
631 rat pairs are placed in a social interaction arena (23.5cm W × 44.45cm L × 27cm H clear plastic
632 bin with Sani-chip bedding) and allowed to interact for 30min. Both Observers and
633 Demonstrators are returned to their home cages and food is withheld for 23hr prior to the social

634 interaction. For the social interaction, Demonstrators are given the opportunity to consume one
635 of two flavors of powdered chow (flavored with 2% marjoram or 0.5% thyme; counterbalanced
636 according to group assignments) for 30min in a room separate from Observers. Our pilot studies
637 and previous published work (62, 63) show that rats equally prefer these flavors of chow. The
638 Demonstrator rat is then placed in the social interaction arena with the Observer rat, and the pairs
639 are allowed to socially interact for 30min. Observers are then returned to their home cage and
640 allowed to eat *ad libitum* for 1h and then food is removed. The following day, the 23h food-
641 deprived Observer animals are given a home cage food preference test for either the flavor of
642 chow paired with the Demonstrator animal, or a novel, unpaired flavor of chow that is a flavor
643 that was not given to the Demonstrator animal (2% marjoram vs. 0.5% thyme; counterbalanced
644 according to group assignments). All animals received an ICV 18mmol infusion of CNO (2uL
645 total volume) 1h prior to the social interaction session, rendering only DREADDs animals
646 chemogenetically inactivated by CNO. Food intake (1h) was recorded with spillage accounted
647 for by collecting crumbs onto Techboard paper that is placed under the cages of each animal.
648 The % preference for the paired flavor is calculated as: 100*Demonstrator-paired flavored chow
649 intake/Demonstrator + Novel flavored chow intake. In this procedure, normal untreated animals
650 learn to prefer the Demonstrator paired flavor based on social interaction and smelling the breath
651 of the Demonstrator rat (28, 39, 61-63). A diagram of the STFP procedure is included in Fig. 3E.
652
653 **Zero maze**
654 The zero maze behavioral paradigm was used to evaluate anxiety-like behavior. The zero
655 maze apparatus used was an elevated circular track, divided into four equal length sections. Two
656 zones were open with 3 cm high curbs ('open zones'), whereas the two other zones were closed
657 with 17.5 cm high walls ('closed zones'). All animals received an ICV 18mmol infusion of CNO
658 (2uL total volume) 1h prior to testing, rendering only DREADDs animals chemogenetically
659 inactivated by CNO. Behavioral testing was performed during the light cycle. Animals were
660 placed in the maze for a single, 5min trial in which the location of the center of the animal's
661 body was measured by AnyMaze Behavior Tracking Software (Stoelting, Wood Dale, IL). The
662 apparatus was cleaned with 10% ethanol in between animals. During the trial, the number of
663 open zone entries and total time spent in open sections (defined as body center in open sections)

664 were measured, which are each indicators of anxiety-like behavior in this procedure. A diagram
665 of the zero maze apparatus is included in Fig. 3G.
666
667 **Open field**
668 An open field test was used to evaluate general levels of locomotor activity. The
669 apparatus used for the open field test was an opaque gray plastic bin (60cm × 56cm), which was
670 positioned on a flat table in an isolated room with a camera directly above the center of the
671 apparatus. Desk lamps were positioned to provide indirect lighting to all corners of the maze
672 such that the lighting in the box uniformly measured 30 lux throughout. All animals received an
673 ICV 18mmol infusion of CNO (2uL total volume) 1h prior to testing rendering only DREADDs
674 animals chemogenetically inactivated by CNO. Behavioral testing began at dark onset. At the
675 start of the 10min test, each animal was placed in the open field apparatus in the same corner
676 facing the center of the maze. The location of the center of the animal's body was measured with
677 the AnyMaze Behavior Tracking Software (Stoelting, Wood Dale, IL). Total distance traveled
678 was measured by tracking movement from the center of the animal's body throughout the test.
679
680 **Identification of collateral targets of CA1v to LS projecting neurons**
681 Collateral targets of the CA1v to LS neural pathway were identified using a dual viral
682 approach (diagram of approach in Fig. 4A) where a retrograde vector was injected into the LS
683 (AAV2retro-hSyn1-eGFP-2A-iCre-WPRE; 200nL per side; coordinates as above), and a Cre-
684 dependent anterograde vector (AAV1-CAG-Flex-tdTomato-WPRE-bGH; 200nL per side;
685 coordinates as above) was injected in the CA1v. This latter injection drives tdTomato transgene
686 expression in CA1v neurons that project to the LS, which allows for brain-wide analyses of
687 collateral targets. After 3 weeks of incubation time to allow for complete transduction and
688 expression of the viruses, brains were collected, immunohistochemically processed, and imaged
689 as described below.
690
691 **cFOS + FISH neurotransmitter phenotyping of LS neurons engaged during appetitive**
692 **spatial memory testing**
693 Activation of LS neurons from the spatial memory probe test was confirmed with c-Fos
694 immunoreactivity analyses. Animals receiving the DREADDs-mediated treatment for reversible

695 inactivation of CA1v to LS signaling underwent training in the appetitive food seeking memory
696 task (conducted as described above). One hour before the memory probe, animals received ICV
697 injection of CNO (n=4) or vehicle (n=4). Animals were tested in the memory probe and perfused
698 with tissue harvest 90 min later. Fluorescent *in situ* hybridization analyses for c-Fos, ChAT,
699 GAD1, and vGLUT2 [source] were performed, and co-localization of c-Fos positive cells and
700 individual neurotransmitter markers was quantitatively analyzed for the rats (n=4) in the vehicle
701 treated group.
702
703 **Identification of second-order targets of CA1v to LS projecting neurons**
704 To identify second order targets of CA1v to LS-projecting neurons (diagram of approach
705 in Fig. 5A), animals received a bilateral injection of a transsynaptic Cre-inducing anterograde
706 vector into CA1v (AAV1-hSyn-Cre-WPRE-hGH; 200nL per side; coordinates as above) that
707 drives expression of Cre in both first-order (CA1v injection site) and 2nd-order (but not 3rd-
708 order) neurons via transsynaptic virion release (45, 64). This was combined with a bilateral
709 injection of a Cre-dependent anterograde vector in the LS (AAV1-CAG-Flex-tdTomato-WPRE-
710 bGH; 200nL per side, coordinates as above). This latter injection allows for anterograde tracing
711 from 1st-order LS targets receiving synaptic input from CA1v. After 3 weeks of incubation time
712 to allow for complete transduction and expression of the viruses, brains were collected,
713 immunohistochemically processed, and imaged as described below.
714 Data were entered using a custom built data-entry platform (Axiome C, created by JDH)
715 built around Microsoft Excel software and designed to facilitate entry of data points for all gray
716 matter regions across their atlas levels as described in a rat brain reference atlas: Brain Maps 4.0
717 (57). The Axiome C approach was used previously to facilitate the analysis of brain gene-
718 expression data (65). An ordinal scale, ranging from 0 (absent) to 7 (very strong), was used to
719 record the qualitative weight of anterograde labeling. An average value was then obtained for
720 each region across its atlas levels for which data were available. These data are summarized
721 graphically for a representative animal on a brain flatmap summary diagram (adapted from (66)).
722 The LHA was identified as a primary downstream target of the CA1v to LS pathway
723 from the analyses described above. In order to further confirm this conclusion, an additional co-
724 injection monosynaptic neural tracing strategy (COIN; (44, 45)) was conducted. Animals (n=6)
725 received unilateral pressure injections of AAV1-GFP (AAV1-hSyn-eGFP-WPRE-bGH;

726 Addgene) targeting the CA1v and, in the same animal, fluorogold (Fluorochrome) targeting the
727 LHA (injection coordinates described above). Following a 10-day incubation period, animals
728 were fixation-perfused and tissue was collected and processed as described below. Injection sites
729 were confined to the CA1v (AAV1) and LHA (FG) in the same animal ("double hits", n=4).
730 Appositions between FG and GFP were examined in the LS in these animals by visualizing
731 native GFP and GF fluorescence.
732
733 **Immunohistochemistry**
734 Rats were anesthetized via an intramuscular injection of an anesthesia cocktail (ketamine
735 90mg/kg BW xylazine, 2.8mg/kg BW and acepromazine and 0.72mg/kg BW) then transcardially
736 perfused with 0.9% sterile saline (pH 7.4) followed by 4% paraformaldehyde (PFA) in 0.1M
737 borate buffer (pH 9.5; PFA). Brains were dissected from the skull and post-fixed in PFA with
738 15% sucrose for 24h, then flash frozen in isopentane cooled in dry ice. Brains were sectioned to
739 30µm thickness on a freezing microtome. Sections were collected in 5-series and stored in
740 antifreeze solution at −20°C until further processing. General fluorescence IHC labeling
741 procedures were performed as follows. The antibodies and dilutions that were used are as
742 follows: [1] For lesion histology using the neuron-specific protein NeuN, the rabbit anti-NeuN
743 primary antibody (1:1000, Abcam) was used followed by a donkey anti-rabbit conjugated to
744 AF488 (1:500, Jackson Immunoresearch). [2] To amplify the native tdTomato signal for
745 neuroanatomical tracing or DREADDs histology, the rabbit anti-RFP primary antibody (1:2000,
746 Rockland) was used followed by a donkey anti-rabbit conjugated to Cy3 (1:500, Jackson
747 Immunoresearch). [3] To amplify the native GFP signal for LS injection site histology, the
748 chicken anti-GFP primary antibody (1:500, Abcam) was used followed by a donkey anti-chicken
749 secondary antibody conjugated to AF488 (1:500, Jackson Immunoresearch). Antibodies were
750 prepared in 0.02M potassium phosphate buffered saline (KPBS) solution containing 0.2% bovine
751 serum albumin and 0.3% Triton X-100 at 4°C overnight. After thorough washing with 0.02M
752 KPBS, sections were incubated in secondary antibody solution. All secondary antibodies were
753 obtained from Jackson Immunoresearch and used at 1:500 dilution at 4°C, with overnight
754 incubations (Jackson Immunoresearch; West Grove, PA, USA). Sections were mounted and
755 coverslipped using 50% glycerol in 0.02 M KPBS and the edges were sealed with clear nail

polish. Photomicrographs were acquired using a Nikon 80i (Nikon DSQI1,1280X1024 resolution, 1.45 megapixel) under epifluorescence or darkfield illumination.
Lesions and virus expression were quantified in one out of five series of brain tissue sections and analyses were performed in sections from Swanson Brain Atlas level 34-36 (57). The inclusion / exclusion criteria are described above in the methods of each of these experiments.

Statistics

Data are expressed as mean +/- SEM. Differences were considered to be statistically significant at $p<0.05$. All variables were analyzed using the advanced analytics software package Statistica (StatSoft, Tulsa, OK, USA). For all measures of food intake, body weight, and errors/latency during spatial foraging and spatial escape task training, differences between groups were evaluated using two-way repeated measures ANOVAs (treatment x time). For lesion experiments, measures during spatial foraging and spatial escape task probes, differences between groups were evaluated using two-tailed independent two-sample Student's t-tests. For CA1v to LS disconnection experiments, measures during spatial foraging and spatial escape task probes, the STFP paradigm, the zero maze paradigm, and the open field test, differences between groups were evaluated using one-way ANOVAs. Significant ANOVAs were analyzed with a Fisher's LSD posthoc test where appropriate. Outliers were identified as being more extreme than the median +/- 1.5 * interquartile range. For all experiments, assumptions of normality, homogeneity of variance (HOV), and independence were met where required.

ACKNOWLEDGEMENTS

This work was supported by National Institute of Diabetes and Digestive and Kidney Diseases grants: DK104897 to SEK, DK118944 to CML, and DK116558 to ANS. Clozapine-N-Oxide was kindly provided by the National Institute of Mental Health. The authors are grateful to the Kanoski lab undergraduate research assistants for their assistance in behavioral experiments and histology.

COMPETING INTERESTS

There are not competing interests to declare.

Figure 1

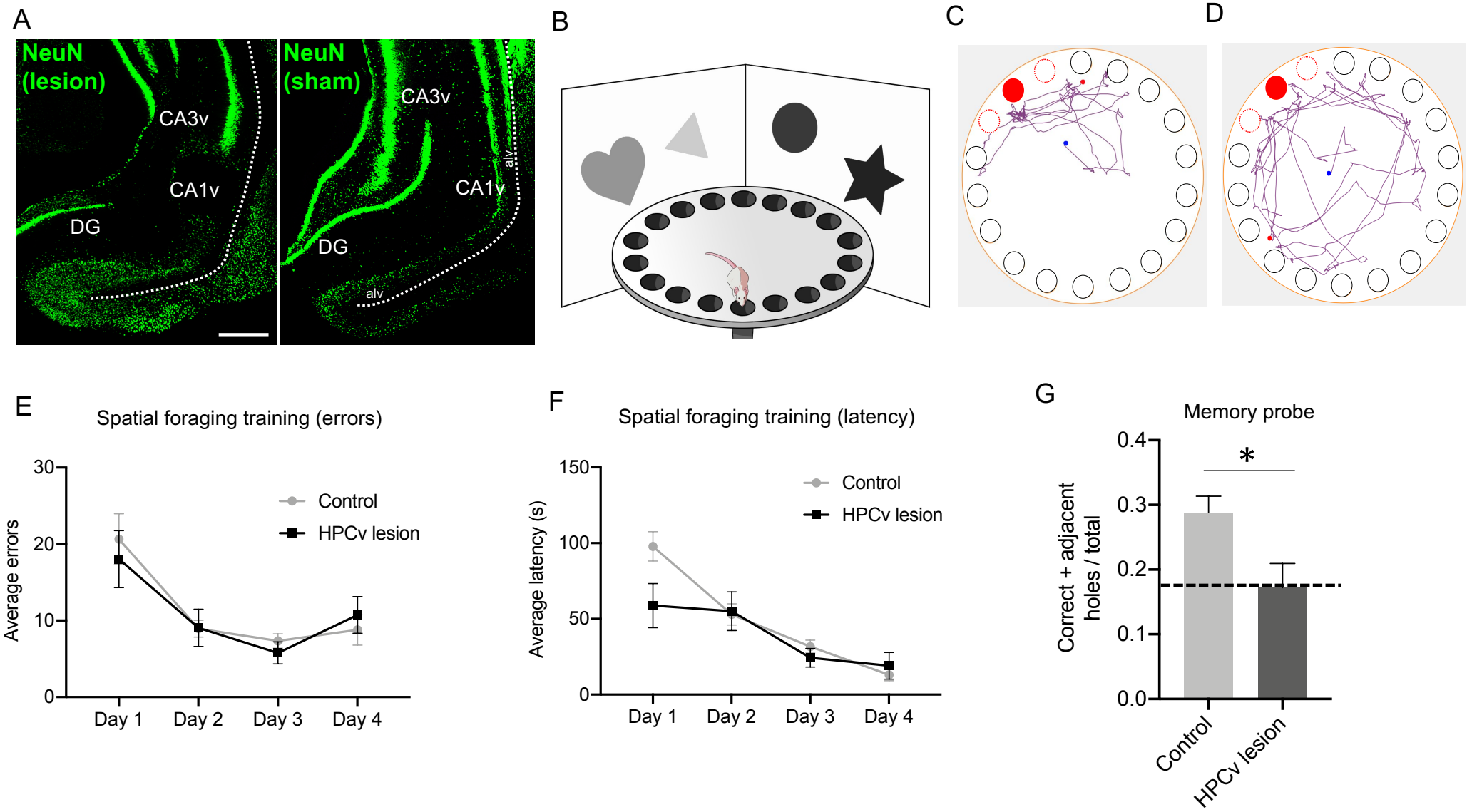
A
NeuN (lesion)
CA3v
CA1v
DG
NeuN (sham)
CA3v
CA1v
DG
alv
alv
B
C
D
E
Spatial foraging training (errors)
Average errors
30
20
10
0
Control
HPCv lesion
Day 1
Day 2
Day 3
Day 4
F
Spatial foraging training (latency)
Average latency (s)
150
100
50
0
Control
HPCv lesion
Day 1
Day 2
Day 3
Day 4
G
Memory probe
Correct + adjacent holes / total
0.4
0.3
0.2
0.1
0.0
*
Control
HPCv lesion

789 **Figure 1. Bilateral HPCv lesions impair spatial memory for food location.** Representative
790 HPCv lesion histology with NeuN immunohistochemistry (A; scale bars 500μm). Spatial
791 foraging task apparatus (B). Representative navigation paths of a control animal preferentially
792 investigating correct (filled red) and adjacent holes (outlined orange) during spatial foraging
793 memory probe (C). Representative navigation path of HPCv lesioned animal during spatial
794 foraging memory probe (D). Bilateral HPCv lesions did not impair learning of the spatial
795 foraging task compared to controls, as measured by errors before locating correct hole during
796 task training (E) and latency to locate correct hole during task training (F). Bilateral HPCv
797 lesions impaired retention of the spatial foraging task, as measured by the ratio of investigation
798 of correct plus adjacent holes over total investigated during the first minute of the task ($p<0.05$;
799 G). Dotted line indicates chance performance level (0.167). For graphs 1D-G, lesion n = 11,
800 control n = 18. All values expressed as mean +/- SEM.
801
802

Figure 2

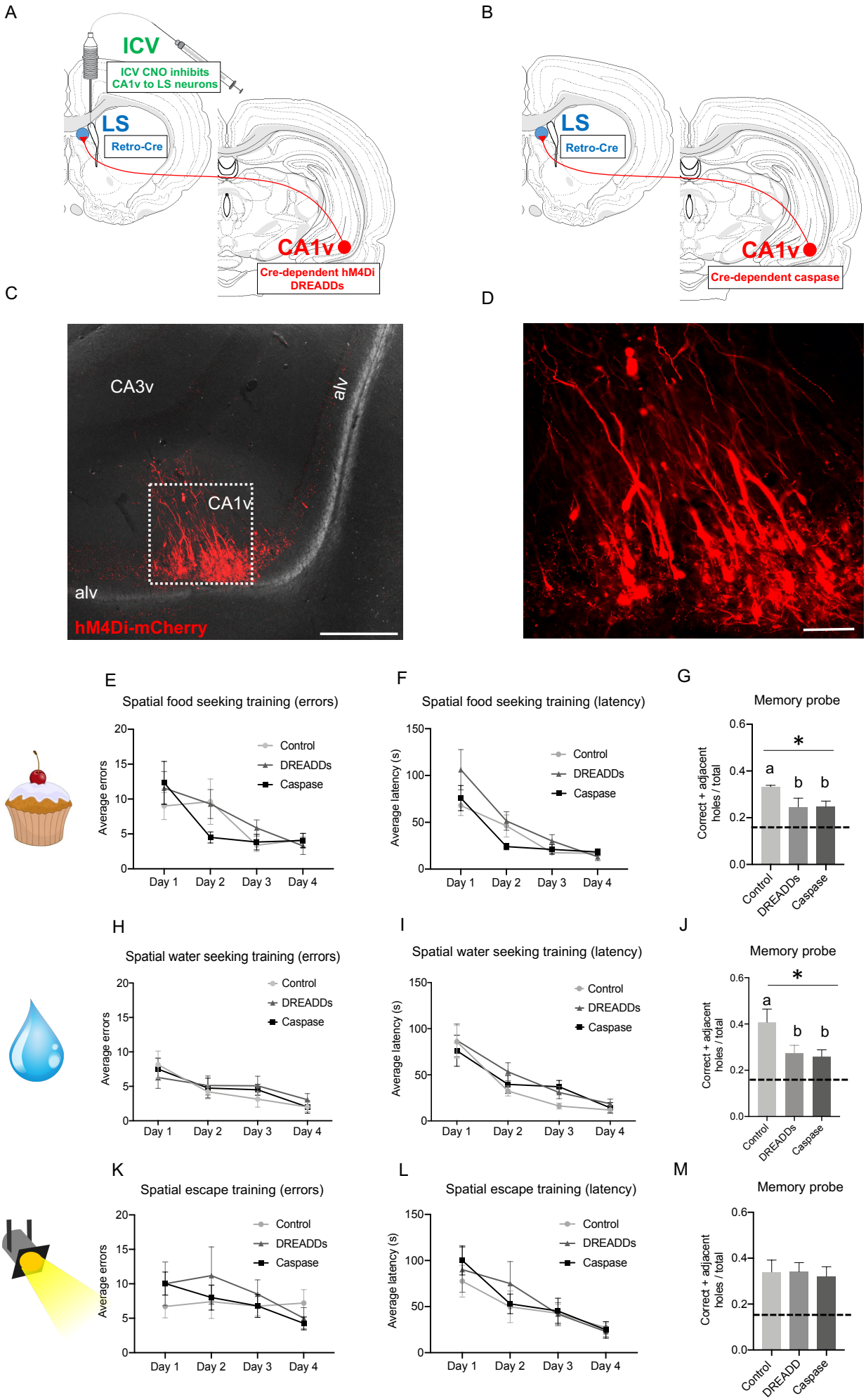
A
ICV
ICV CNO inhibits CA1v to LS neurons
LS
Retro-Cre
CA1v
Cre-dependent hM4Di DREADDs
B
LS
Retro-Cre
CA1v
Cre-dependent caspase
C
CA3v
alv
CA1v
alv
hM4Di-mCherry
D
E
Spatial food seeking training (errors)
Average errors
Control
DREADDs
Caspase
Day 1
Day 2
Day 3
Day 4
F
Spatial food seeking training (latency)
Average latency (s)
G
Memory probe
Correct + adjacent holes / total
a
b
b
Control
DREADDs
Caspase
H
Spatial water seeking training (errors)
I
Spatial water seeking training (latency)
J
Memory probe
K
Spatial escape training (errors)
L
Spatial escape training (latency)
M
Memory probe
DREADD

Figure 2. Reversible and chronic CA1v to LS neural disconnection impairs spatial memory for food and water location but not for escape location. Diagram of dual viral approach using a cre-dependent inhibitory DREADDs (AAV-hSyn-DIO-hM4D(Gi)-mCherry) approach to reversibly disconnect CA1v to LS neural pathway (with CNO injected 1hr before memory probe) (A). Diagram of dual viral approach using a cre-dependent caspase (AAV1-Flex-taCasp3-TEVp) approach to chronically disconnect CA1v to LS neural pathway (B). Representative injection site in CA1v demonstrating LS-projecting neurons infected with inhibitory DREADDs, which simultaneously drives expression of a fluorescent mCherry transgene (C, D; scale bars 500µm and 100µm, respectively). Neither reversible (DREADDs) nor chronic (caspase) disconnection of the CA1v to LS pathway impaired learning of the spatial food seeking task compared to controls, as measured by errors before correct hole during task training (E) and latency to correct hole during task training (F). Both reversible and chronic disconnection of the CA1v to LS pathway impaired retention of the food location as measured by the ratio of investigation of correct plus adjacent holes over total investigations during entire two minutes of the task ($p<0.05$; G). Likewise, reversible (DREADDs) and chronic (caspase) disconnection of the CA1v to LS pathway did not impair learning of the spatial water seeking task compared to controls, as measured by errors before correct hole during task training (H) and latency to correct hole during task training (I), but impaired memory retention of the water location during the probe (J). In contrast, disconnection of the CA1v to LS pathway either reversibly (DREADDs) or chronically (caspase) did not impair performance on the spatial escape task. There were no differences in learning as measured by errors before correct hole during task training (K) and latency to correct hole during task training (L). Unlike the spatial foraging task, retention of the spatial escape task was not impaired by reversible nor chronic disconnection of the CA1v to LS pathway (M). For graphs 2E-G (CA1v to LS disconnect cohort 1), DREADDs n=6, caspase n=10, control n=8. For graphs 2H-J (CA1v to LS disconnect cohort 3), DREADDs n=8, caspase n=8, control n=7). For graphs 2K-M (CA1v to LS disconnect cohort 2), DREADDs n=8, caspase n=12, control n=10. Dotted line indicates chance performance level (0.167). All values expressed as mean +/- SEM.

Figure 3

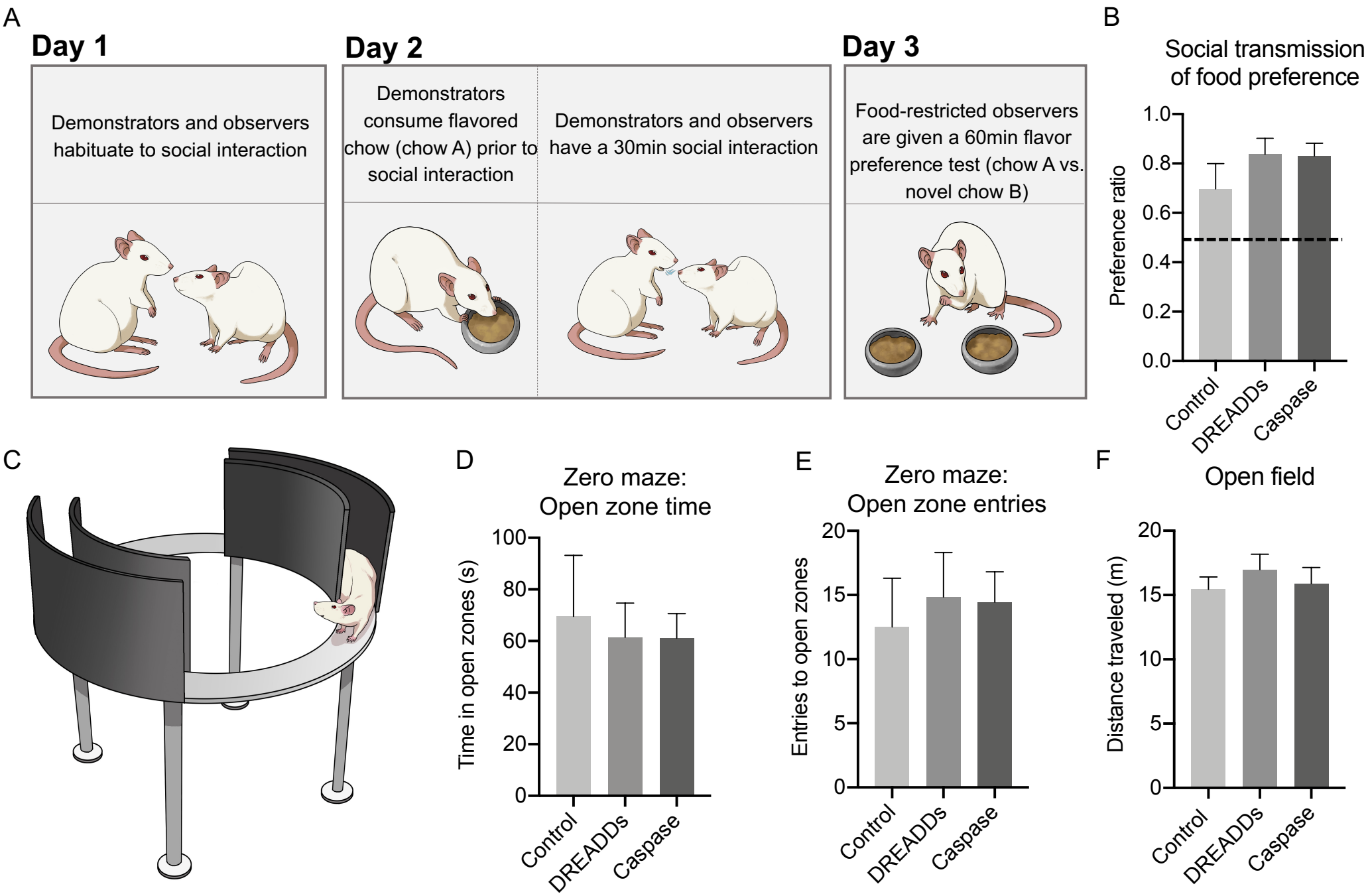
A
Day 1
Demonstrators and observers habituate to social interaction
Day 2
Demonstrators consume flavored chow (chow A) prior to social interaction
Demonstrators and observers have a 30min social interaction
Day 3
Food-restricted observers are given a 60min flavor preference test (chow A vs. novel chow B)
B
Social transmission of food preference
Preference ratio
1.0
0.8
0.6
0.4
0.2
0.0
Control
DREADDs
Caspase
C
D
Zero maze: Open zone time
Time in open zones (s)
100
80
60
40
20
0
Control
DREADDs
Caspase
E
Zero maze: Open zone entries
Entries to open zones
20
15
10
5
0
Control
DREADDs
Caspase
F
Open field
Distance traveled (m)
20
15
10
5
0
Control
DREADDs
Caspase

832 **Figure 3. Neither reversible nor chronic CA1v to LS neural disconnection impair spatial**
833 **memory for escape location, social transmission of food preference, anxiety-like behavior,**
834 **or general locomotor activity levels.** Diagram of the social transmission of food preference
835 (STFP) task (A). Neither reversible nor chronic disconnection of the CA1v to LS pathway impair
836 STFP learning compared to controls, as measured by a food preference ratio (B), with the dotted
837 line indicating chance preference level (0.50). Diagram of the zero maze apparatus (C). Anxiety-
838 like behavior was not influenced by reversible or chronic disconnection of the CA1v to LS
839 pathway compared to controls, as measured by performance in the zero maze task, specifically
840 time in open zones (D) and entries into open zones (E). Neither chronic nor reversible CA1v to
841 LS disconnection affected open field performance compared to controls, as measured by total
842 distance traveled (F). For graphs 3B, 3D, and 3E (CA1v to LS disconnect cohort 1), DREADDs
843 n=6, caspase n=10, control n=8. For graph 3F (CA1v to LS disconnect cohort 2), DREADDs
844 n=8, caspase n=12, control n=10. All values expressed as mean +/- SEM.
845
846

Figure 4

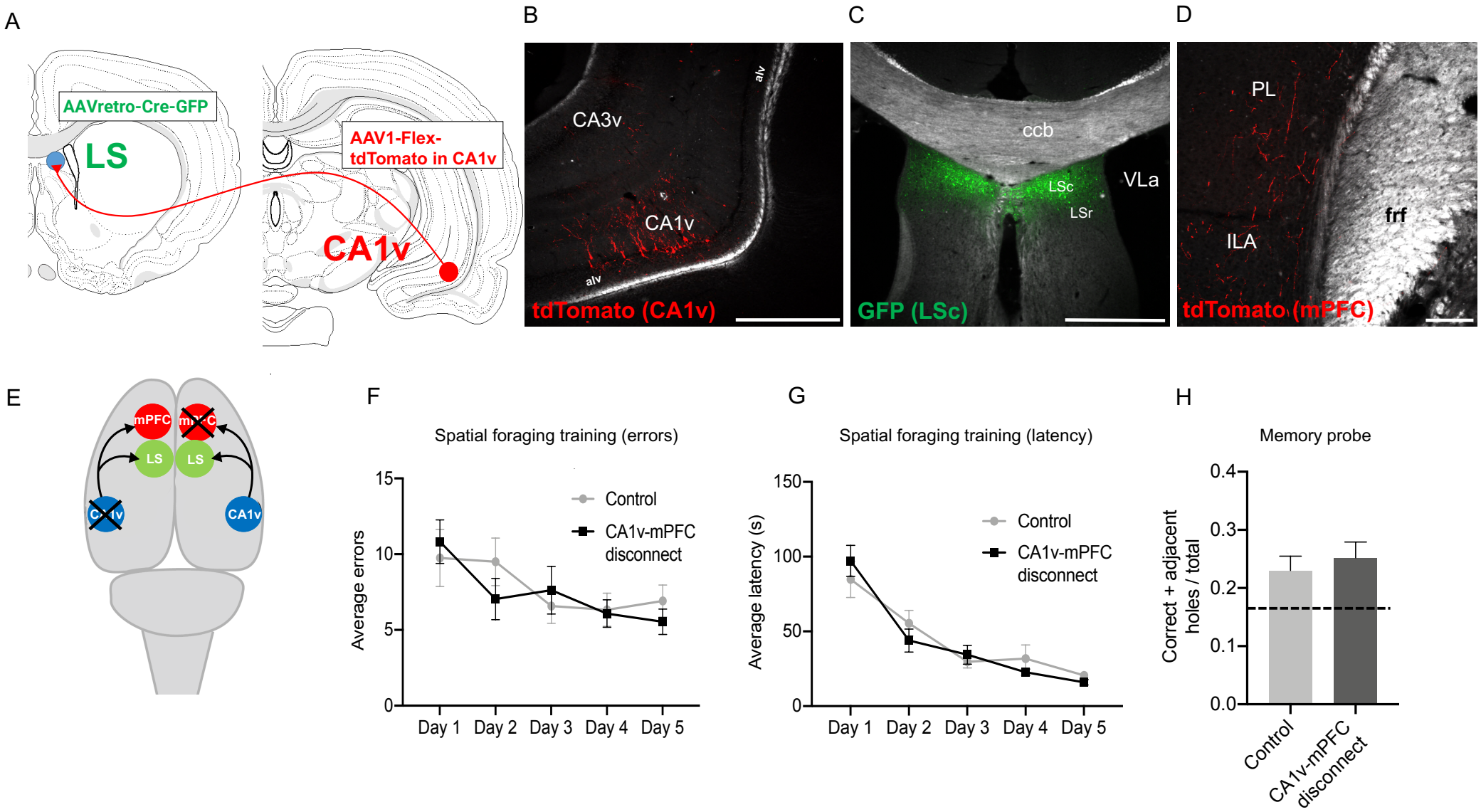
A
AAVretro-Cre-GFP
LS
AAV1-Flex-
tdTomato in CA1v
CA1v
B
CA3v
alv
CA1v
alv
tdTomato (CA1v)
C
ccb
VLa
LSc
LSr
GFP (LSc)
D
PL
frf
ILA
tdTomato (mPFC)
E
mPFC
mPFC
LS
LS
CA1v
CA1v
F
Spatial foraging training (errors)
Average errors
15
10
5
0
Control
CA1v-mPFC
disconnect
Day 1
Day 2
Day 3
Day 4
Day 5
G
Spatial foraging training (latency)
Average latency (s)
150
100
50
0
Control
CA1v-mPFC
disconnect
Day 1
Day 2
Day 3
Day 4
Day 5
H
Memory probe
Correct + adjacent
holes / total
0.4
0.3
0.2
0.1
0.0
Control
CA1v-mPFC
disconnect

847 **Figure 4. CA1v to mPFC disconnection does not impair spatial memory for food location.**
848 Diagram of dual viral approach to identify collateral targets of the CA1v to LS neural pathway
849 (A). Representative CA1v injection site from collateral identification approach (B; scale bar
850 500µm). Representative LS injection site from collateral identification approach (C; scale bar
851 500µm). Representative image collateral axons of the CA1v to LS pathway located in the mPFC
852 (D; scale bar 50µm). Diagram of contralesional approach to functionally disconnect the CA1v to
853 mPFC neural pathway (E). Disconnection of the CA1v to mPFC neural pathway did not
854 influence learning of the spatial foraging task compared to controls, as measured by errors before
855 correct hole during training (F) and latency to correct hole during training (G). Disconnection of
856 the CA1v to mPFC pathway did not influence retention of the spatial foraging task in the
857 memory probe (H). For graphs 4F-H, CA1v to mPFC disconnect n=12, control n=12. All values
858 expressed as mean +/- SEM.
859
860
861

Figure 5

A

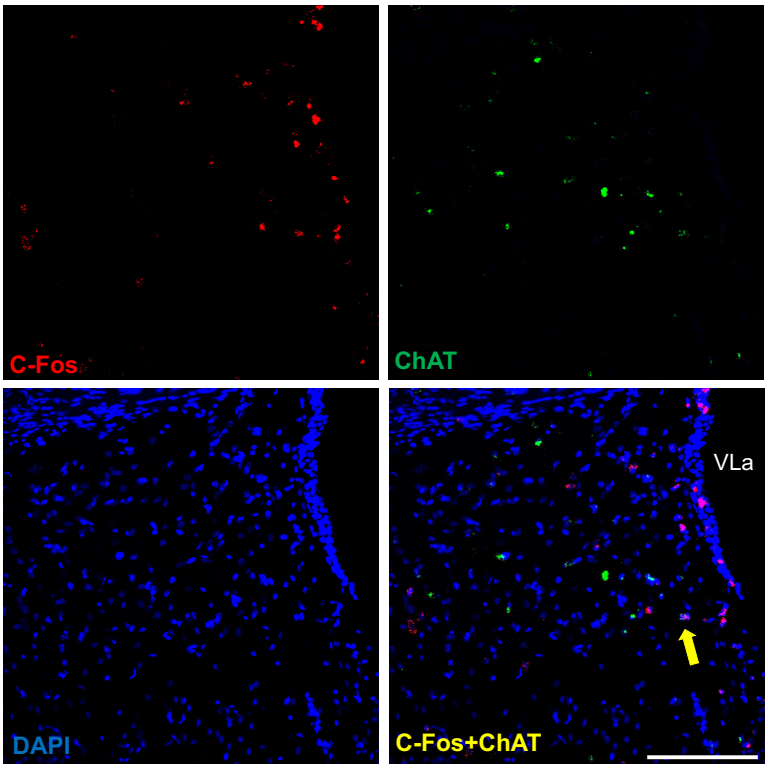

B

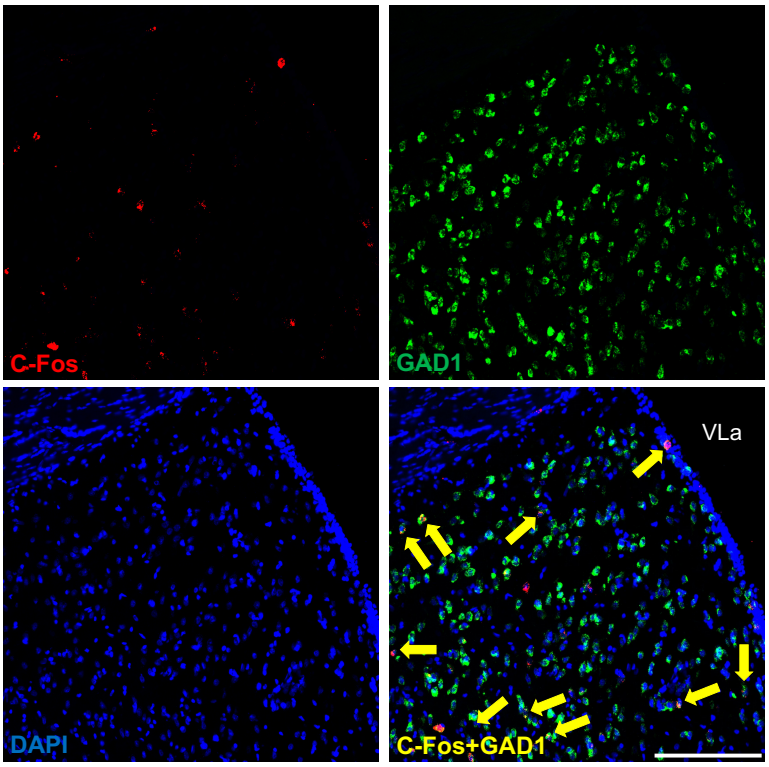

C

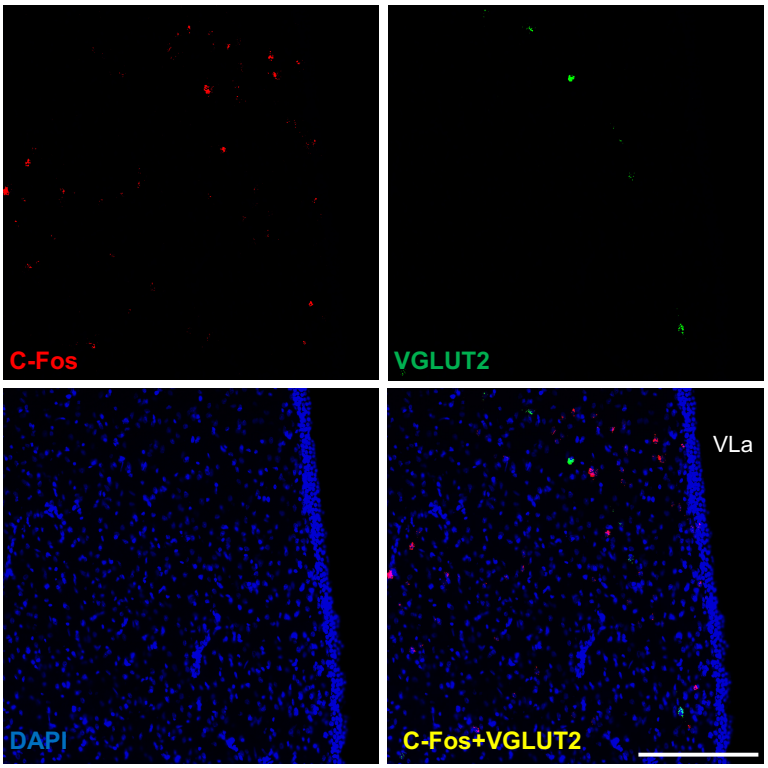

D

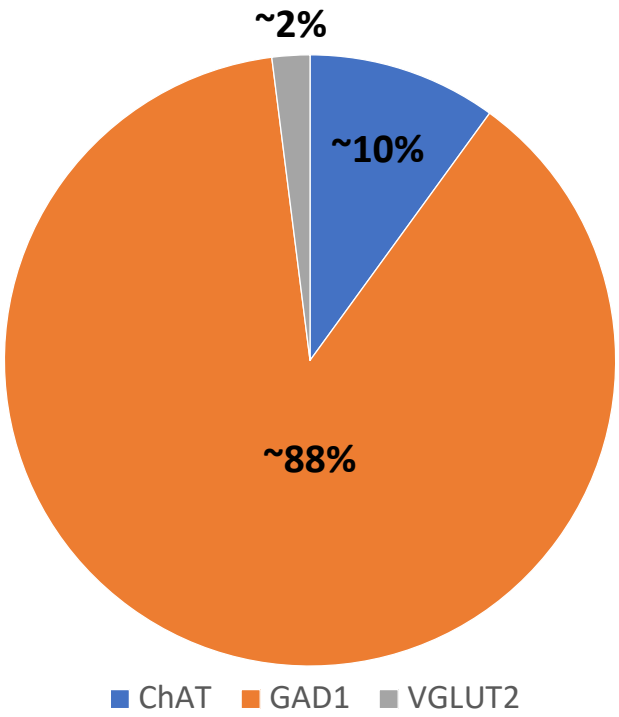

862 **Figure 5. LS neurons activated during food-seeking memory probe are predominantly**
863 **GABAergic.** c-Fos and ChAT colocalization was observed in ~2% of LS neurons (A; scale bar
864 500µm), c-Fos and GAD1 colocalization was observed in ~88% of LS neurons (B; scale bar
865 500µm), and c-Fos and VGLUT2 colocalization was observed in ~10% of LS neurons (C; scale
866 bar 500µm) following the spatial memory probe test (for food reinforcement). For graphs A-C,
867 quantification from DREADDs vehicle group, n=4.
868

Figure 6

A

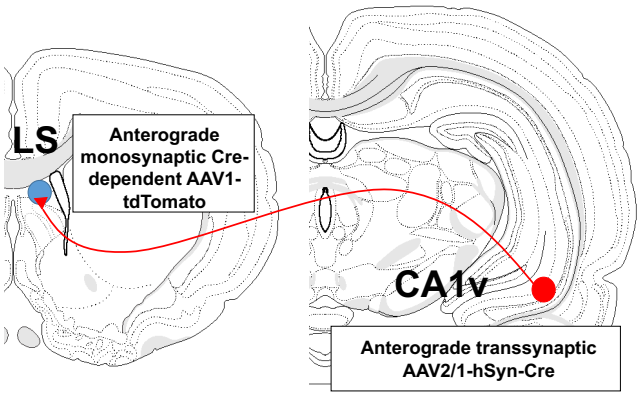

B

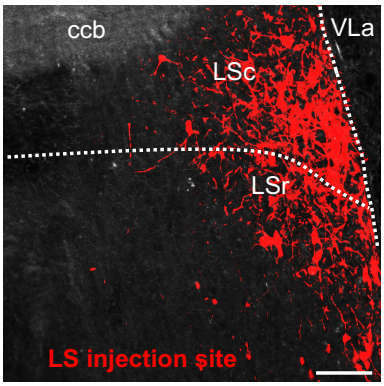

C

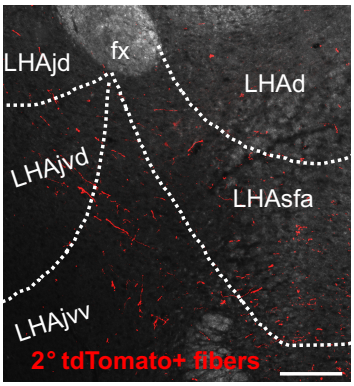

D

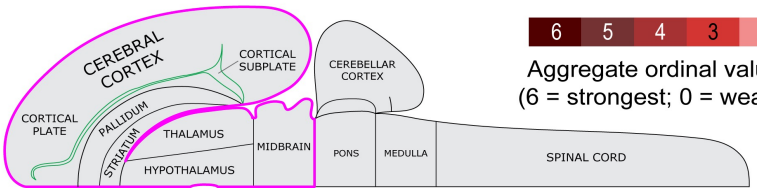

Aggregate ordinal value categories
(6 = strongest; 0 = weakest / absent)

Targeted side (right)

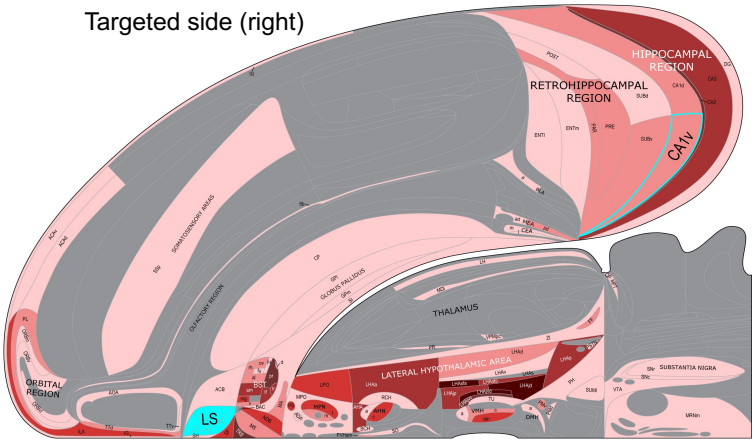

Contralateral side (left)

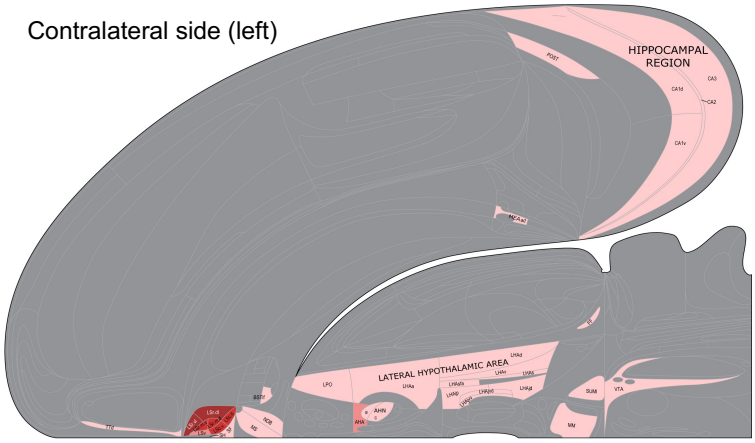

E

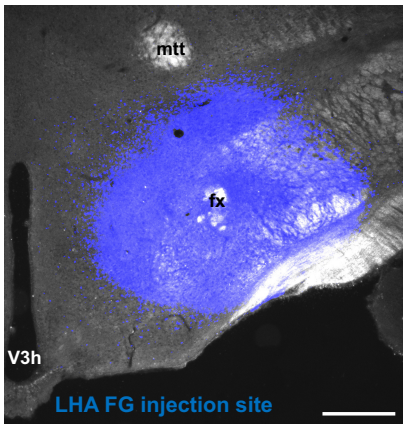

F

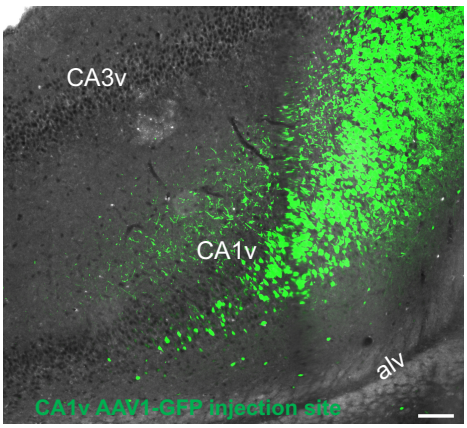

G

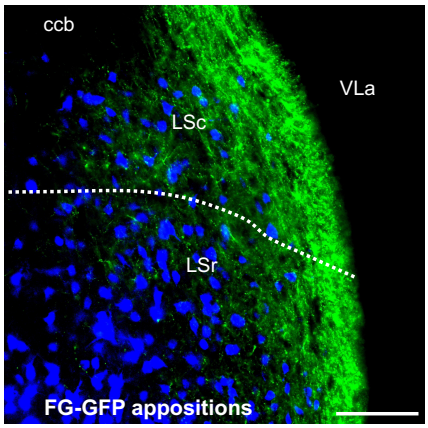

869 **Figure 6. Identification of second-order neural projections downstream of CA1v to LS**
870 **projections.** Diagram of dual viral approach to identify brain regions that are second-order (2°)
871 targets of the CA1v to LS neural pathway (A). Representative LS injection site from second
872 order identification approach (B; scale bar 100µm). Representative image of second-order fibers
873 of the CA1v to LS pathway within the LHA (C; scale bar 200µm). Summary of the projection
874 targets of LS neurons that receive input from CA1v (D; expanded information in Supplementary
875 Table 1). The outputs of the right side of LS neurons receiving CA1v input are represented at the
876 macroscale (gray matter region resolution) on a partial flatmap representation of the rat
877 forebrain, adapted from (66). Connection weights are represented block colors for each region
878 following an ordinal scale ranging from weakest (0 = very weak or absent) to strongest (6 =
879 strong), as there were no 7 (very strong) values. The inset at lower left represents one side of the
880 brain with the part represented in the upper diagrams outlined in magenta. The COIN approach
881 for further confirmation of second-order tracing strategy is depicted with FG injection site in the
882 LHA (E; scale bar 500µm), representative AAV1-GFP injection site in the CA1v (F; scale bar
883 100µm), and FG-GFP appositions in the LS (G; scale bar 100µm).
884
885

Supplemental Figure 1

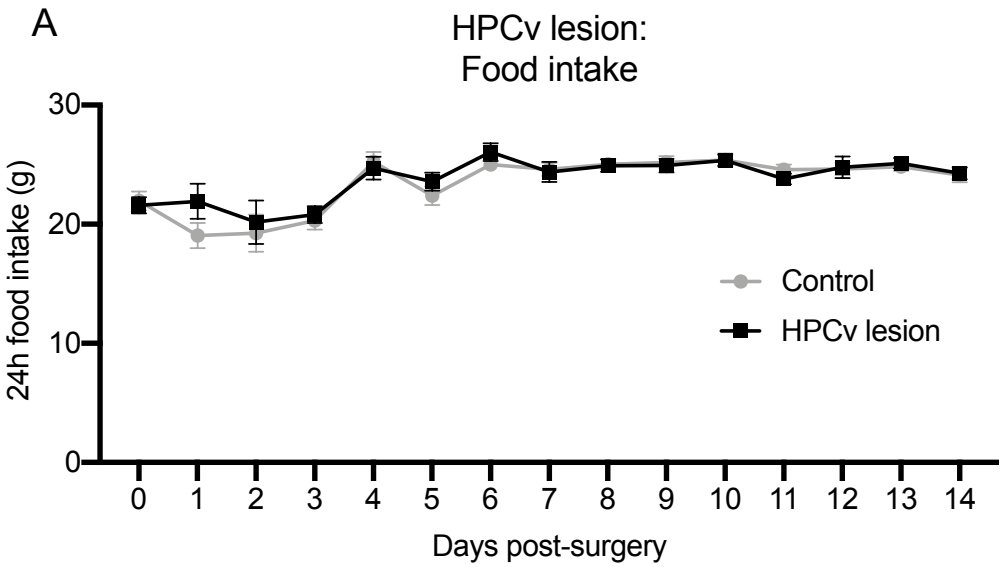

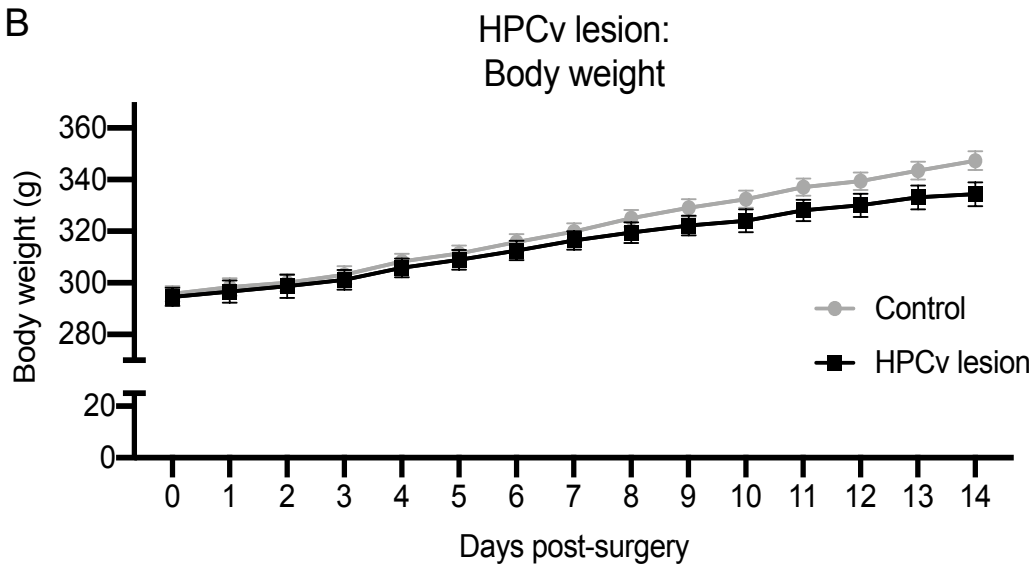

886 **Supplementary Figure 1. Effect of bilateral HPCv lesions on food intake and body weight.**
887 There were no effects on food intake (A) or body weight (B) of bilateral HPCv lesions compared
888 to controls. Lesion n = 11, control n = 18. All values expressed as mean +/- SEM.
889
890

Supplemental Figure 2

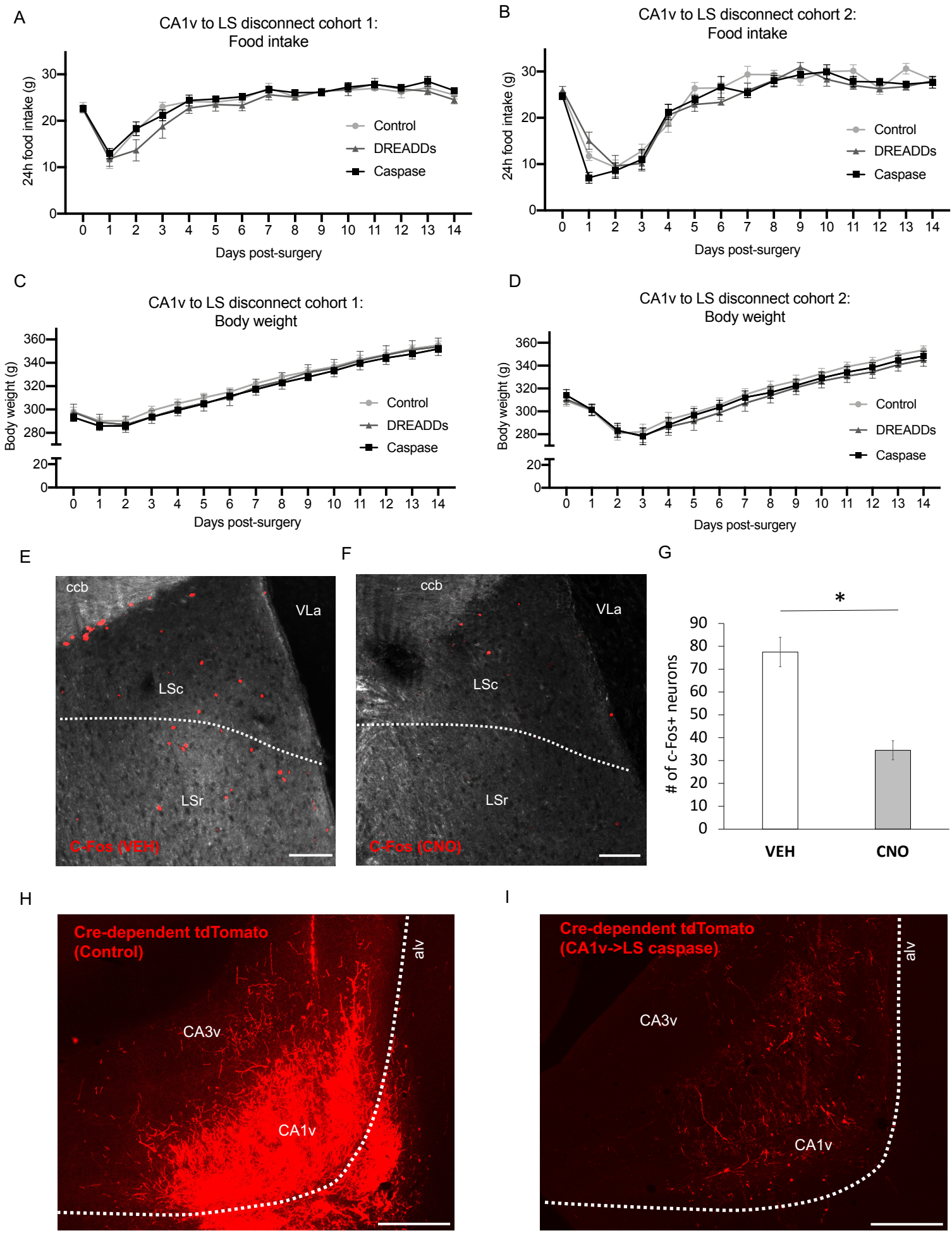

891 **Supplementary Figure 2. Effect of reversible and chronic disconnection of the CA1v to LS**
892 **neural pathway on food intake and body weight, and verification of the acute and chronic**
893 **approach.** There were no effects on food intake (cohort 1: A; cohort 2: B) or body weight
894 (cohort 1: C; cohort 2: D) of reversible (DREADDs) or chronic (caspase) disconnection of the
895 CA1v to LS neural pathway compared to controls. Histological verification of inhibitory
896 DREADDs-induced acute silencing of LS-projecting CA1v neurons determines that the
897 appetitive spatial memory probe induces c-Fos activation in the LS in vehicle-treated animals
898 (E), an outcome significantly reduced in CNO-treated animals (F, G). Histological verification of
899 caspase-induced chronic silencing of the LS-projecting CA1v neurons demonstrates that cre-
900 dependent tdTomato labeling of CA1v neurons induced by LS-origin retro-cre is robust in a
901 control animal (H), but substantially reduced in an animal injected with cre-dependent caspase
902 combined with cre-dependent tdTomato due to caspase-induced cell death (I). For graphs S2A-B
903 (CA1v to LS disconnect cohort 1), DREADDs n=6, caspase n=10, control n=8. For graphs S2C-
904 D (CA1v to LS disconnect cohort 2), DREADDs n=8, caspase n=12, control n=10. For graphs
905 S2E-G, DREADDs vehicle n=4, DREADDs CNO n=4. For graphs S2H-I, caspase n=6, control
906 n=2). All values expressed as mean +/- SEM.
907
908

Supplemental Figure 3

Chronic Disconnection of the vCA1-LS Pathway

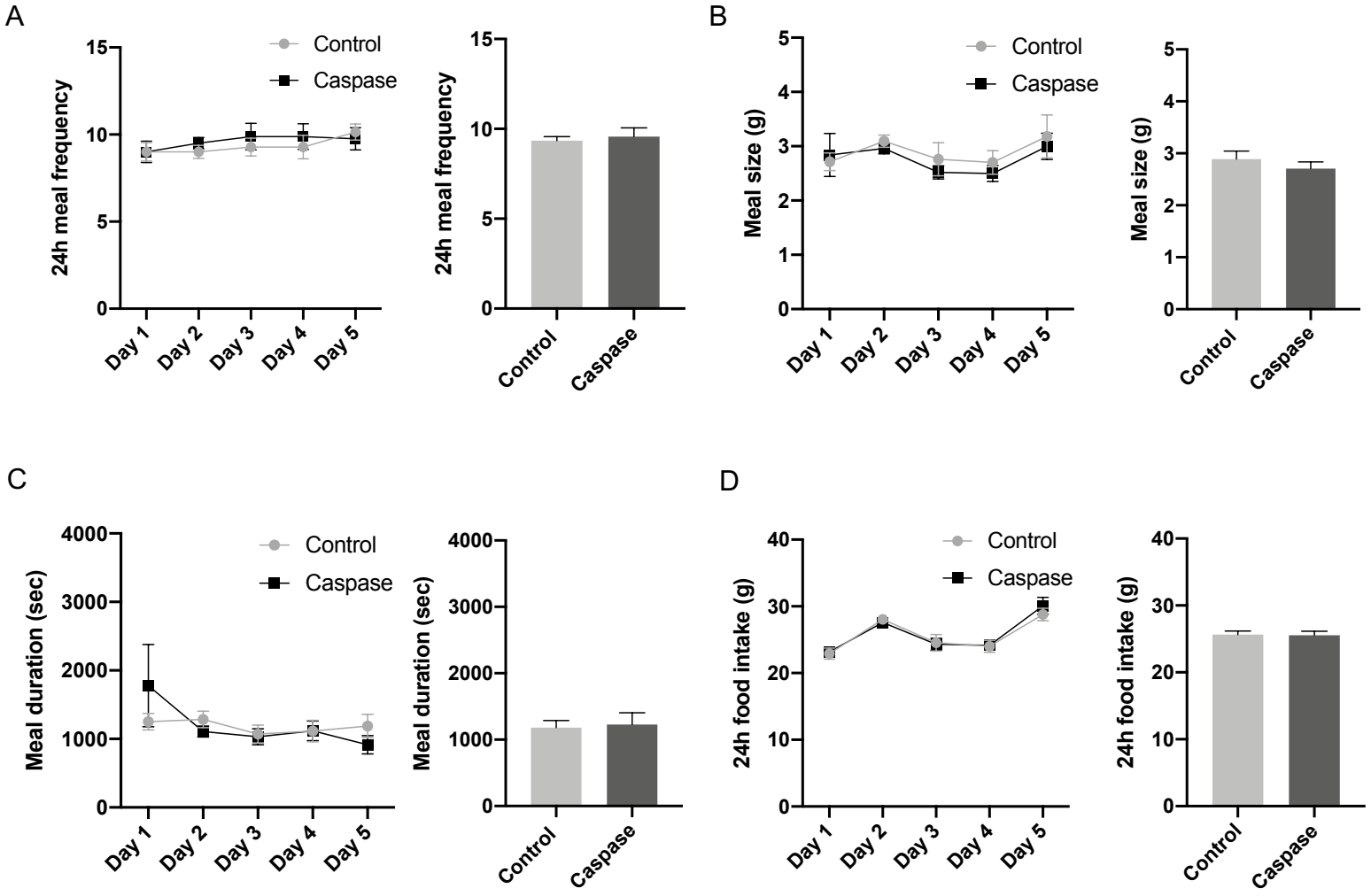

Acute Disconnection of the vCA1-LS Pathway

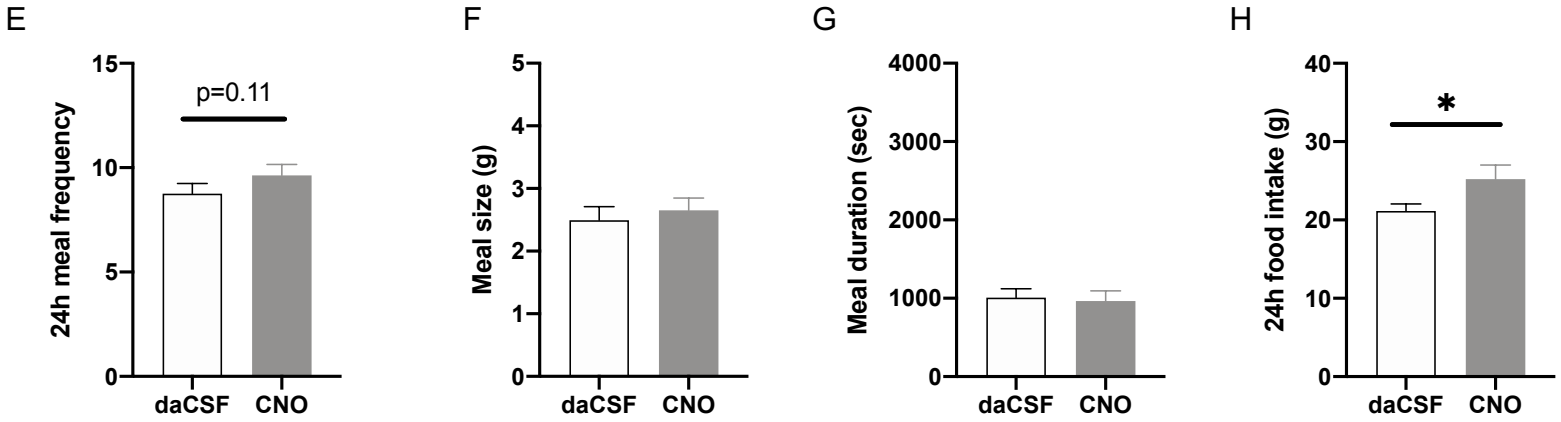

909 **Supplementary Figure 3. Effect of reversible and chronic disconnection of CA1v to LS**
910 **neural pathway on feeding behavior.** Compared with control animals, chronic caspase-
911 mediated disconnection of the CA1v to LS pathway did not significantly affect meal frequency
912 (A), meal size (B), meal duration (C), or 24h cumulative food intake (D) over the course of the
913 5-day recording period. Acute DREADDs-mediated disconnection of the CA1v to LS pathway
914 (via CNO infusion) resulted in non-significant trend towards increased meal frequency (E), no
915 differences in meal size (F) or meal duration (G), and a significant increase in 24h cumulative
916 food intake (H) in comparison with vehicle injection. For graphs S3A-D, caspase n=7 and
917 control n=7. For graphs S3E-H, DREADDs n=8 (within-subjects). All values expressed as mean
918 +/- SEM.
919
920

Supplemental Figure 4

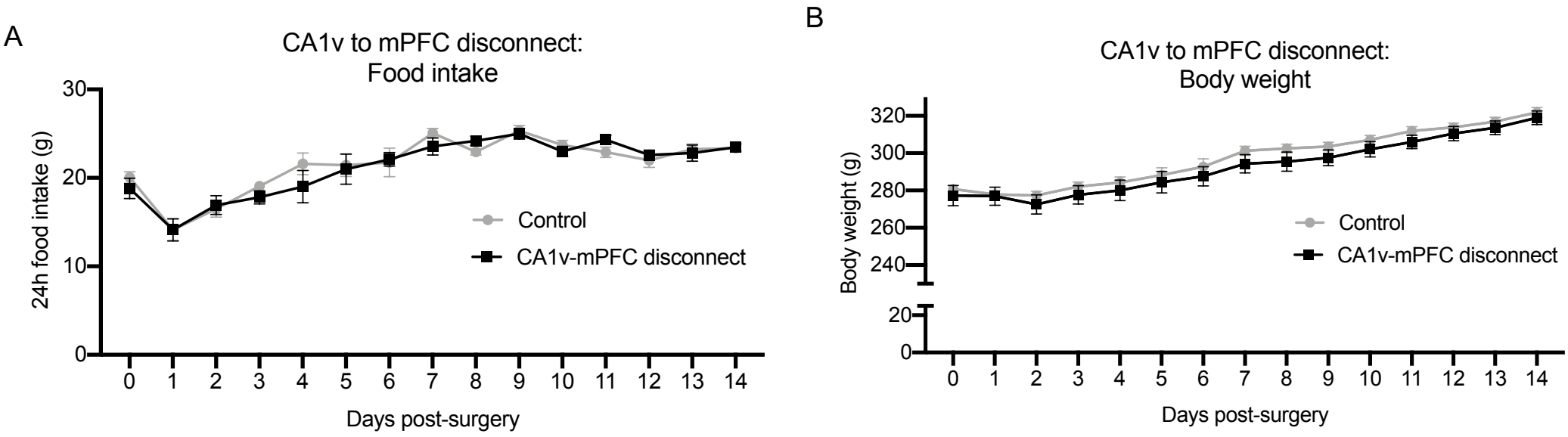

921 **Supplementary Figure 4. Effect of contralesional disconnection methods on food intake and**
922 **body weight.** There were no effects on food intake (A) or body weight (B) of contralesional
923 CA1v to mPFC compared to controls. CA1v to mPFC disconnect n=12, control n=12. All values
924 expressed as mean +/- SEM.
925
926

Supplementary Table 1

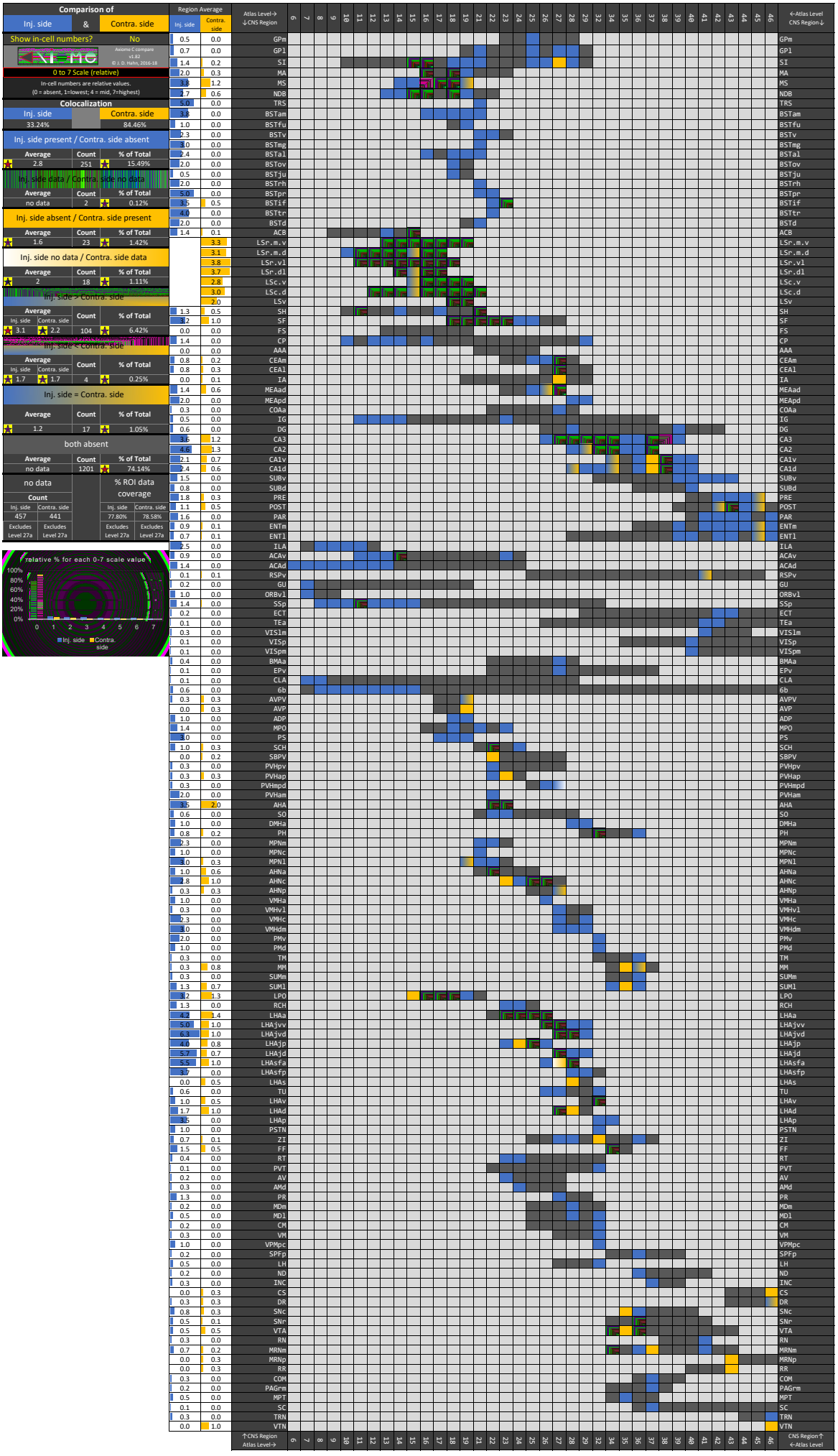

927 **Supplementary Table 1.** Summary table of the forebrain projection targets of LS neurons that
928 receive input from CA1v (derived the same raw data as the brain flatmap summary diagram in
929 Fig. 6D).
930
931

REFERENCES

1. R. G. M. Morris, U. Frey, "Hippocampal synaptic plasticity: Role in spatial learning or the automatic recording of attended experience?" in Burgess, Neil (Ed); Jeffery, Kathryn J (Ed); et al (1999) The hippocampal and parietal foundations of spatial cognition. (Oxford University Press, U Edinburgh, Ctr for Neuroscience, Edinburgh, Scotland London, 1999), pp. 220-246.
2. D. C. Rowland, Y. Roudi, M. B. Moser, E. I. Moser, Ten Years of Grid Cells. *Annu Rev Neurosci* **39**, 19-40 (2016).
3. R. Morris, Developments of a water-maze procedure for studying spatial learning in the rat. *Journal of neuroscience methods* **11**, 47-60 (1984).
4. C. A. Barnes, Memory deficits associated with senescence: a neurophysiological and behavioral study in the rat. *J Comp Physiol Psychol* **93**, 74-104 (1979).
5. J. O'Keefe, J. Dostrovsky, The hippocampus as a spatial map: preliminary evidence from unit activity in the freely-moving rat. *Brain research* (1971).
6. T. Hafting, M. Fyhn, S. Molden, M. B. Moser, E. I. Moser, Microstructure of a spatial map in the entorhinal cortex. *Nature* **436**, 801-806 (2005).
7. M. S. Fanselow, H.-W. Dong, Are the dorsal and ventral hippocampus functionally distinct structures? *Neuron* **65**, 7-19 (2010).
8. A. T. Keinath *et al.*, Precise spatial coding is preserved along the longitudinal hippocampal axis. *Hippocampus* **24**, 1533-1548 (2014).
9. K. B. Kjelstrup *et al.*, Finite scale of spatial representation in the hippocampus. *Science* **321**, 140-143 (2008).
10. L. de Hoz, J. Knox, R. G. Morris, Longitudinal axis of the hippocampus: both septal and temporal poles of the hippocampus support water maze spatial learning depending on the training protocol. *Hippocampus* **13**, 587-603 (2003).
11. J. Ferbinteanu, C. Ray, R. J. McDonald, Both dorsal and ventral hippocampus contribute to spatial learning in Long-Evans rats. *Neurosci Lett* **345**, 131-135 (2003).
12. M. B. Moser, E. I. Moser, Functional differentiation in the hippocampus. *Hippocampus* **8**, 608-619 (1998).
13. S. E. Kanoski, H. J. Grill, Hippocampus Contributions to Food Intake Control: Mnemonic, Neuroanatomical, and Endocrine Mechanisms. *Biol Psychiatry* **81**, 748-756 (2017).
14. P. G. Henke, Hippocampal pathway to the amygdala and stress ulcer development. *Brain Res Bull* **25**, 691-695 (1990).
15. K. G. Kjelstrup *et al.*, Reduced fear expression after lesions of the ventral hippocampus. *Proceedings of the National Academy of Sciences* **99**, 10825-10830 (2002).
16. S. Gaskin, A. Gamliel, M. Tardif, E. Cole, D. G. Mumby, Incidental (unreinforced) and reinforced spatial learning in rats with ventral and dorsal lesions of the hippocampus. *Behav Brain Res* **202**, 64-70 (2009).
17. M. S. Bienkowski *et al.*, Integration of gene expression and brain-wide connectivity reveals the multiscale organization of mouse hippocampal networks. *Nat Neurosci* **21**, 1628-1643 (2018).

18. R. Hannapel *et al.*, Postmeal Optogenetic Inhibition of Dorsal or Ventral Hippocampal Pyramidal Neurons Increases Future Intake. *eNeuro* **6** (2019).
19. R. C. Hannapel, Y. H. Henderson, R. Nalloor, A. Vazdarjanova, M. B. Parent, Ventral hippocampal neurons inhibit postprandial energy intake. *Hippocampus* **27**, 274-284 (2017).
20. B. K. Mani *et al.*, Neuroanatomical characterization of a growth hormone secretagogue receptor-green fluorescent protein reporter mouse. *J Comp Neurol* **522**, 3644-3666 (2014).
21. J. M. Zigman, J. E. Jones, C. E. Lee, C. B. Saper, J. K. Elmquist, Expression of ghrelin receptor mRNA in the rat and the mouse brain. *J Comp Neurol* **494**, 528-548 (2006).
22. I. Merchenthaler, M. Lane, P. Shughrue, Distribution of pre-pro-glucagon and glucagon-like peptide-1 receptor messenger RNAs in the rat central nervous system. *J Comp Neurol* **403**, 261-280 (1999).
23. S. E. Kanoski, S. M. Fortin, K. M. Ricks, H. J. Grill, Ghrelin Signaling in the Ventral Hippocampus Stimulates Learned and Motivational Aspects of Feeding via PI3K-Akt Signaling. *Biol Psychiatry* **73**, 915-923 (2013).
24. S. E. Kanoski *et al.*, Hippocampal leptin signaling reduces food intake and modulates food-related memory processing. *Neuropsychopharmacology* **36**, 1859-1870 (2011).
25. T. M. Hsu *et al.*, A hippocampus to prefrontal cortex neural pathway inhibits food motivation through glucagon-like peptide-1 signaling. *Molecular psychiatry* **23**, 1555-1565 (2018).
26. T. M. Hsu, J. D. Hahn, V. R. Konanur, A. Lam, S. E. Kanoski, Hippocampal GLP-1 receptors influence food intake, meal size, and effort-based responding for food through volume transmission. *Neuropsychopharmacology* **40**, 327-337 (2015).
27. A. N. Suarez, C. M. Liu, A. M. Cortella, E. E. Noble, S. E. Kanoski, Ghrelin and Orexin Interact to Increase Meal Size Through a Descending Hippocampus to Hindbrain Signaling Pathway. *Biol Psychiatry* **87**, 1001-1011 (2020).
28. T. M. Hsu *et al.*, Hippocampus ghrelin receptor signaling promotes socially-mediated learned food preference. *Neuropharmacology* **131**, 487-496 (2018).
29. G. D. Petrovich, N. S. Canteras, L. W. Swanson, Combinatorial amygdalar inputs to hippocampal domains and hypothalamic behavior systems. *Brain research reviews* **38**, 247-289 (2001).
30. C. De La Rosa-Prieto *et al.*, Subicular and CA1 hippocampal projections to the accessory olfactory bulb. *Hippocampus* **19**, 124-129 (2009).
31. L. W. Swanson, W. M. Cowan, An autoradiographic study of the organization of the efferent connections of the hippocampal formation in the rat. *J Comp Neurol* **172**, 49-84 (1977).
32. A. Arszovszki, Z. Borhegyi, T. Klausberger, Three axonal projection routes of individual pyramidal cells in the ventral CA1 hippocampus. *Front Neuroanat* **8**, 53 (2014).
33. P. Y. Risold, L. W. Swanson, Structural evidence for functional domains in the rat hippocampus. *Science* **272**, 1484-1486 (1996).
34. P. Sweeney, Y. Yang, An excitatory ventral hippocampus to lateral septum circuit that suppresses feeding. *Nature communications* **6**, 10188 (2015).

1017 35. R. Garcia, R. M. Vouimba, R. Jaffard, Spatial discrimination learning induces LTP-like
1018 changes in the lateral septum of mice. *Neuroreport: An International Journal for the*
1019 *Rapid Communication of Research in Neuroscience* **5**, 329-332 (1993).
1020 36. R. Jaffard, R. M. Vouimba, A. Marighetto, R. Garcia, Long-term potentiation and long-
1021 term depression in the lateral septum in spatial working and reference memory. *J*
1022 *Physiol Paris* **90**, 339-341 (1996).
1023 37. S. J. Terrill *et al.*, Nucleus accumbens melanin-concentrating hormone signaling
1024 promotes feeding in a sex-specific manner. *Neuropharmacology* **178**, 108270 (2020).
1025 38. A. Carballo-Marquez, A. Vale-Martinez, G. Guillazo-Blanch, M. Marti-Nicolovius,
1026 Muscarinic receptor blockade in ventral hippocampus and prelimbic cortex impairs
1027 memory for socially transmitted food preference. *Hippocampus* **19**, 446-455 (2009).
1028 39. R. A. Countryman, N. L. Kaban, P. J. Colombo, Hippocampal c-fos is necessary for long-
1029 term memory of a socially transmitted food preference. *Neurobiol Learn Mem* **84**, 175-
1030 183 (2005).
1031 40. G. M. Parfitt *et al.*, Bidirectional Control of Anxiety-Related Behaviors in Mice: Role of
1032 Inputs Arising from the Ventral Hippocampus to the Lateral Septum and Medial
1033 Prefrontal Cortex. *Neuropsychopharmacology : official publication of the American*
1034 *College of Neuropsychopharmacology* **42**, 1715-1728 (2017).
1035 41. N. L. Trent, J. L. Menard, The ventral hippocampus and the lateral septum work in
1036 tandem to regulate rats' open-arm exploration in the elevated plus-maze. *Physiology &*
1037 *behavior* **101**, 141-152 (2010).
1038 42. J. C. Jimenez *et al.*, Anxiety Cells in a Hippocampal-Hypothalamic Circuit. *Neuron* **97**,
1039 670-683.e676 (2018).
1040 43. T. M. Hsu *et al.*, Hippocampus ghrelin signaling mediates appetite through lateral
1041 hypothalamic orexin pathways. *eLife* **4** (2015).
1042 44. R. H. Thompson, L. W. Swanson, Hypothesis-driven structural connectivity analysis
1043 supports network over hierarchical model of brain architecture. *Proc Natl Acad Sci U S A*
1044 **107**, 15235-15239 (2010).
1045 45. A. N. Suarez *et al.*, Gut vagal sensory signaling regulates hippocampus function through
1046 multi-order pathways. *Nature communications* **9**, 2181 (2018).
1047 46. M. S. Fanselow, H. W. Dong, Are the dorsal and ventral hippocampus functionally
1048 distinct structures? *Neuron* **65**, 7-19 (2010).
1049 47. M. Contreras, T. Pelc, M. Llofriu, A. Weitzenfeld, J. M. Fellous, The ventral hippocampus
1050 is involved in multi-goal obstacle-rich spatial navigation. *Hippocampus* **28**, 853-866
1051 (2018).
1052 48. S. L. T. Lee, D. Lew, V. Wickenheisser, E. J. Markus, Interdependence between dorsal and
1053 ventral hippocampus during spatial navigation. *Brain Behav* **9**, e01410 (2019).
1054 49. D. Olivo, M. Caba, F. Gonzalez-Lima, J. F. Rodríguez-Landa, A. A. Corona-Morales,
1055 Metabolic activation of amygdala, lateral septum and accumbens circuits during food
1056 anticipatory behavior. *Behavioural brain research* **316**, 261-270 (2017).
1057 50. M. Carus-Cadavieco *et al.*, Gamma oscillations organize top-down signalling to
1058 hypothalamus and enable food seeking. *Nature* **542**, 232-236 (2017).

1059 51. S. J. Terrill *et al.*, Role of lateral septum glucagon-like peptide 1 receptors in food intake.
1060 *American journal of physiology. Regulatory, integrative and comparative physiology* **311**,
1061 R124-132 (2016).
1062 52. S. J. Terrill, K. D. Wall, N. D. Medina, C. B. Maske, D. L. Williams, Lateral septum growth
1063 hormone secretagogue receptor affects food intake and motivation for sucrose
1064 reinforcement. *American journal of physiology. Regulatory, integrative and comparative*
1065 *physiology* **315**, R76-r83 (2018).
1066 53. C. Wang, C. M. Kotz, Urocortin in the lateral septal area modulates feeding induced by
1067 orexin A in the lateral hypothalamus. *American journal of physiology. Regulatory,*
1068 *integrative and comparative physiology* **283**, R358-367 (2002).
1069 54. J. Hauser, L. H. Llano López, J. Feldon, P. A. Gargiulo, B. K. Yee, Small lesions of the dorsal
1070 or ventral hippocampus subregions are associated with distinct impairments in working
1071 memory and reference memory retrieval, and combining them attenuates the
1072 acquisition rate of spatial reference memory. *Hippocampus* **30**, 938-957 (2020).
1073 55. D. S. Olton, The radial arm maze as a tool in behavioral pharmacology. *Physiology &*
1074 *behavior* **40**, 793-797 (1987).
1075 56. X. Zhao *et al.*, Orexin-A-induced ERK1/2 activation reverses impaired spatial learning and
1076 memory in pentylenetetrazol-kindled rats via OX1R-mediated hippocampal
1077 neurogenesis. *Peptides* **54**, 140-147 (2014).
1078 57. L. W. Swanson, Brain maps 4.0-Structure of the rat brain: An open access atlas with
1079 global nervous system nomenclature ontology and flatmaps. *J Comp Neurol* **526**, 935-
1080 943 (2018).
1081 58. R. C. Ritter, P. G. Slusser, S. Stone, Glucoreceptors controlling feeding and blood glucose:
1082 location in the hindbrain. *Science* **213**, 451-452 (1981).
1083 59. E. E. Noble *et al.*, Hypothalamus-hippocampus circuitry regulates impulsivity via
1084 melanin-concentrating hormone. *Nat Commun* **10**, 4923 (2019).
1085 60. L. E. Herzog *et al.*, Interaction of Taste and Place Coding in the Hippocampus. *The*
1086 *Journal of neuroscience : the official journal of the Society for Neuroscience* **39**, 3057-
1087 3069 (2019).
1088 61. R. A. Countryman, P. E. Gold, Rapid forgetting of social transmission of food preferences
1089 in aged rats: relationship to hippocampal CREB activation. *Learn Mem* **14**, 350-358
1090 (2007).
1091 62. B. G. Galef, Jr., W. Y. Lee, E. E. Whiskin, Lack of interference in long-term memory for
1092 socially learned food preferences in rats (Rattus norvegicus). *J Comp Psychol* **119**, 131-
1093 135 (2005).
1094 63. B. G. Galef, Jr., E. E. Whiskin, Socially transmitted food preferences can be used to study
1095 long-term memory in rats. *Learn Behav* **31**, 160-164 (2003).
1096 64. B. Zingg *et al.*, AAV-Mediated Anterograde Transsynaptic Tagging: Mapping
1097 Corticocollicular Input-Defined Neural Pathways for Defense Behaviors. *Neuron* **93**, 33-
1098 47 (2017).
1099 65. J. D. Hahn, O. Sporns, A. G. Watts, L. W. Swanson, Macroscale intrinsic network
1100 architecture of the hypothalamus. *Proc Natl Acad Sci U S A* **116**, 8018-8027 (2019).

66. J. D. Hahn, Swanson, L. W,. Bowman, I., Foster, N. N., Zingg, B., Bienkowski, M. S., Hintiryan, H., & Dong, H.-W. , An open access mouse brain flatmap and upgraded rat and human brain flatmaps based on current reference atlases. *J. Comp. Neurol.* (2020).